



# Electron-Nucleus Interactions And Their Biophysical Consequences

Ivano Bertini<sup>1</sup> and Claudio Luchinat<sup>2</sup>

<sup>1</sup>Department of Chemistry, University of Florence, Via G. Capponi, 7, 50121 Florence, Italy, and

<sup>2</sup>Department of Soil Science and Plant Nutrition, University of Florence, P.le delle Cascine 7, 50144 Florence, Italy

## 1. Basic electron spin properties

1.1. Differences and analogies between electron and nuclear spins

## 2. Electron-nucleus interactions seen from the nucleus

2.1. The shifts

2.2. Nuclear relaxation

## 3. Gains and losses from the NMR viewpoint

## 4. Solvent relaxometry

## 5. Paramagnetic ions as probes

5.1. Shift reagents

5.2. Relaxation reagents

5.3. Contrast agents in MRI

## 6. Magnetic coupled systems

# Electron-nucleus interactions and their biophysical consequences

## 1. Basic electron spin properties

Free electrons possess an angular momentum and a magnetic moment. These properties are accounted for on the basis of the spin formalism <sup>1</sup>. The spin wavefunction is represented by the  $|s, m_s\rangle$  wavefunction where the spin quantum number  $s$  is  $1/2$  and  $m_s$  is  $-1/2$  or  $+1/2$ .

The intensity of the magnetic moment of a free electron is

$$\mu = |g_e| \sqrt{s(s+1)} \mu_B = 20023 \sqrt{1/2(1/2+1)} \mu_B \quad (1)$$

where  $g_e$  is the Lande factor, which expresses the proportionality between angular and magnetic moments and  $\mu_B$ , the Bohr magneton, represents the conventional unit of measurement of magnetic moments on a microscopic scale, equal to  $9.2741 \times 10^{-24} \text{ JT}^{-1}$ . The factor  $g_e$  is conventionally taken as positive. The vector magnetic moment aligns in a magnetic field  $B_0$  according to its  $m_s$  value (**Figure 1**). The magnetic moment vector  $\mu$  of intensity as from **Equation 1** has allowed projections  $\mu_z$  along it equal to  $-1/2 g_e \mu_B$  ( $m_s = -1/2$ ) and  $1/2 g_e \mu_B$  ( $m_s = 1/2$ ) along  $B_0$ .

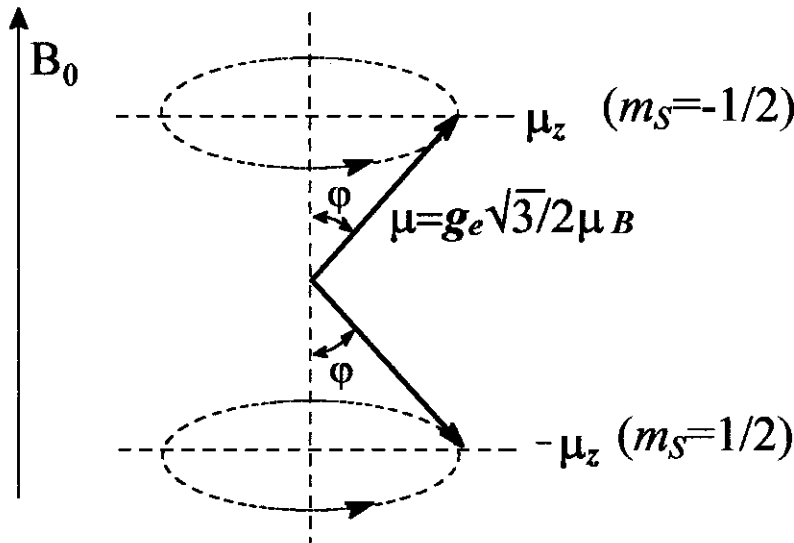


Figure 1. Allowed orientations of a single electron magnetic moment  $\mu$  in an external magnetic field  $B_0$ .  $\mu$  precesses about  $B_0$  as indicated by the arrows. An ensemble of electron magnetic moments gives rise to a cone of vectors, randomly oriented, all precessing with the same frequency.

The direction of the magnetic moment is not known; actually, classical physics ensures that a magnetic moment forming an angle  $\varphi$  with the direction of  $B_0$  precesses along  $B_0$  with a frequency  $\omega$  such that  $\omega = g_e \mu_B B_0 / \hbar$ . An ensemble of electrons is represented by two cones of vectors. The angles between the magnetic moment and the direction of the external magnetic field will be  $\varphi = \pm 64.34^\circ$ . The two allowed orientations of the magnetic moment differ in energy by  $g_e \mu_B B_0$ . An ensemble of spins in a magnetic field will thus possess a Boltzmann distribution of the two orientations and therefore an induced magnetic moment which is the weighted sum of all magnetic moments in the two orientations.

Often paramagnetic molecules contain more than one unpaired electrons. In this case we describe the system with a total  $S$  spin quantum number such that

$$S = \sum m_s = 1/2 \quad (2)$$

where the sum is over the unpaired electrons. Analogously to the single electron case, every spin property is described by substituting  $s$  with  $S$  and  $m_s$  with  $M_S$ .  $M_S$  has allowed values from  $S$  to  $-S$  with steps of 1<sup>2</sup>.

Up to now the description parallels that of nuclei. However, electrons have an orbital angular momentum and an orbital magnetic moment which are large in free atoms and ions and generally small when the atoms belong to molecules. The interest here is limited to molecules. The orbital contributions to the total angular momentum and magnetic moment depend on many factors among which most important are the ladder of excited states in the molecule and the spin-orbit coupling constant<sup>3</sup>. Such constant expresses the extent of coupling between the spin magnetic moment and the orbital magnetic moment. Along the periodic table it grows from left to right and from top to bottom. In general, if the spin orbit coupling is large (as it is in the case of transition metal ions and much more so in the case of lanthanides) and there are excited states close to the ground state in a molecule, the orbital contribution is relatively large. In some lanthanides, it can be even larger than the spin contribution. A property of the spin magnetic moment, even if the electron is anchored to a molecule, is that it always orients along the external magnetic field and its projection along it,  $\mu_z$  is independent of the orientation of the molecule within the magnetic field.

On the contrary, the orbital contribution has its own orientation within the molecule. The ligand field in a metal ion complex determines the molecular axis along which the orbital magnetic moment is oriented. As a result, the projection of the total electronic magnetic moment along  $B_0$  depends on the orientation of the molecule. Likewise, the intensity of the induced magnetic moment along  $B_0$  depends on the orientation of the molecule and is therefore anisotropic. The induced magnetic moment per unit magnetic field, called magnetic susceptibility ( $\chi$ ), is also anisotropic, and can be represented as a tensor (**Figure 2**).

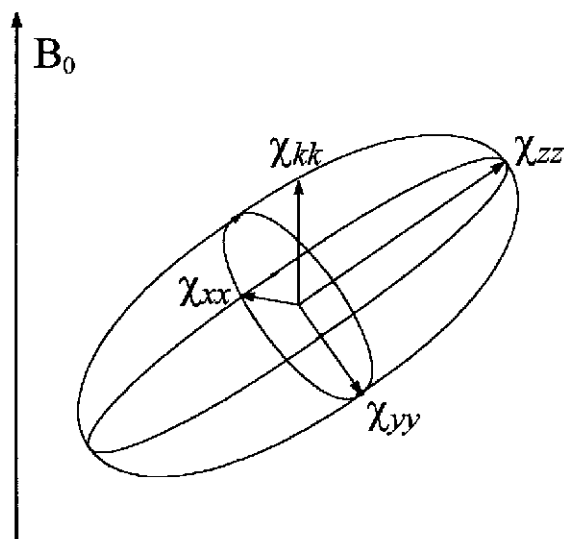


Figure 2. Representation of the magnetic susceptibility tensor  $\chi$ . The magnetic susceptibility is the magnetic moment induced by the external magnetic field divided by the magnetic field. For a generic orientation of the molecule in the magnetic field  $B_0$  the magnetic susceptibility is given by the length of the vector  $\chi_{kk}$ . For the tensor in the example, the magnetic susceptibility is maximal when  $\chi_{zz}$  is along the field, and minimal when  $\chi_{xx}$  is along the field.

In summary, spin-orbit coupling causes the induced magnetic moment and magnetic susceptibility to differ from their spin-only values and to be anisotropic. Spin-orbit coupling has other important consequences:

- i) it accounts for the factor  $g$  being different from the Lande factor  $g_e$  and anisotropic;
- ii) it accounts for the establishment of zero field splitting (ZFS) of spin multiplets; the spin levels with  $S > 1/2$  are split at zero field by spin-orbit and low-symmetry components.

iii) by mixing the spin wavefunction with the orbital wavefunction it allows the electron spin to sense atomic coordinate displacements. Furthermore, such mixing allows electronic transitions (caused by absorption or emission of photons or phonons) which would be forbidden if only the spin were considered.

### 1.1. Differences and analogies between electron and nuclear spins

Analogies between electron and nuclear spins are very many.  $S$  and  $M_S$  spin numbers of the electrons correspond to  $I$  and  $M_I$  spin numbers of the nucleus. The wavefunctions and behavior under spin operators are very similar, i.e.  $|I, M_I\rangle$  corresponds to  $|S, M_S\rangle$ , and

$$\begin{aligned}
 S^2|S, M_S\rangle &= S(S+1)|S, M_S\rangle \\
 I^2|I, M_I\rangle &= I(I+1)|I, M_I\rangle \\
 S_z|S, M_S\rangle &= M_S|S, M_S\rangle \\
 I_z|I, M_I\rangle &= M_I|I, M_I\rangle
 \end{aligned}
 \tag{3}$$

When  $S = 1$ , ZFS may be operative; when  $I = 1$  quadrupolar splitting may occur. Different electronic relaxation times and nuclear relaxation times are operative for different  $M_S$  ( $M_I$ ) levels when  $S$  or  $I$  are larger than 1<sup>4-6</sup>.

Nuclear relaxation occurs through interactions with fluctuating magnetic field components oscillating at the proper frequencies. The same holds for electron relaxation but the effect of such mechanism is overwhelmed by spin-orbit coupling based mechanisms. Rotation, or atomic displacements due for example to solvent collision or to absorption or emission of phonons cause electronic transitions involving different  $M_S$  states. The frequency needed for relaxation of the free electron is 658 times larger than that for the proton (in real systems such ratio may differ from this value). The availability of such frequencies for either nuclear or electron relaxation is given by the corresponding spectral density function,  $J(\omega)$  which is a function of the frequency and of the correlation time relative to the mechanism which causes relaxation<sup>7</sup>.

As far as the nucleus is concerned, we are herein interested in the modulation of the hyperfine interaction energy, i.e. of the coupling energy between the electron and the nucleus. Such modulation may occur through electron relaxation, molecular rotation or chemical exchange. The

frequencies to be considered are zero, the nuclear Zeeman frequency, and the nuclear plus/minus the electron Zeeman frequencies. The spectral density functions are:

$$\begin{aligned}
 J(0) &= \tau_c \\
 J(\omega_I) &= \frac{\tau_c}{1 + \omega_I^2 \tau_c^2} \\
 J(\omega_I - \omega_S) &= J(\omega_I + \omega_S) = \frac{\tau_c}{1 + \omega_S^2 \tau_c^2}
 \end{aligned} \tag{4}$$

where  $\omega$  is the frequency and  $\tau_c$  is the correlation time. A similar approach holds for electron relaxation when the motion causing relaxation spans a "continuous" range of frequencies. This is the case for solution studies and in particular when collision and rotation cause electron relaxation. The spectral densities are:

$$\begin{aligned}
 J(0) &= \tau_v \\
 J(\omega_S) &= \frac{\tau_v}{1 + \omega_S^2 \tau_v^2} \\
 J(2\omega_S) &= \frac{\tau_v}{1 + 4\omega_S^2 \tau_v^2}
 \end{aligned} \tag{5}$$

where the correlation time is indicated as  $\tau_v$ , which is either related to molecular rotation or diffusion. The third term in **Equation 5** contains the frequency  $2\omega_S$ , which corresponds to the  $\Delta M_S = 2$  transition encountered for  $S > 1/2$ . Electron relaxation in solids is related to phonons. Phonons have a particular frequency distribution. In solution at room temperature, if the solid state language is borrowed, the phonons' frequency may be a continuum within a certain range and  $\tau_v$  would be very short.

## 2. Electron-nucleus interactions seen from the nucleus

The interaction between unpaired electrons and nuclei consists of a contact and a dipolar contribution. The contact contribution is due to spin density on the resonating nuclei<sup>8</sup>. It involves the  $s$  orbitals, which have non-zero electron density at the nucleus<sup>9</sup>. Chemical bonds are needed to

transfer spin density. The electron-nucleus contact interaction is therefore analogous to the nucleus-nucleus  $J$ -coupling interaction. The dipolar interaction occurs through space and is again analogous to the nucleus-nucleus dipolar interaction. However, at variance with nuclei, electrons are not point dipoles but are localized at least along several bonds. This tends to complicate the analysis.

## 2.1. The shifts

The contribution to chemical shift due to the presence of unpaired electrons is called hyperfine shift <sup>7</sup>. Sometimes for solutions it is called isotropic shift <sup>10</sup>. It is experimentally determined by subtracting the shift of a diamagnetic analogue from the actual chemical shift. If no diamagnetic analogue is available, the diamagnetic shift can be estimated from first principles, with some approximations. Programs are available to estimate diamagnetic shifts in proteins (see Chapter 10).

The contact shift is relatively simple to describe. The unpaired electron occupies two Zeeman levels with some excess population for  $m_s = -1/2$ . This results in an induced molecular magnetic moment, which is partitioned among all points in space where the unpaired electron is delocalized. In addition, spin polarization mechanisms cause an unpaired spin density contribution on doubly occupied orbitals (**Figure 3**).

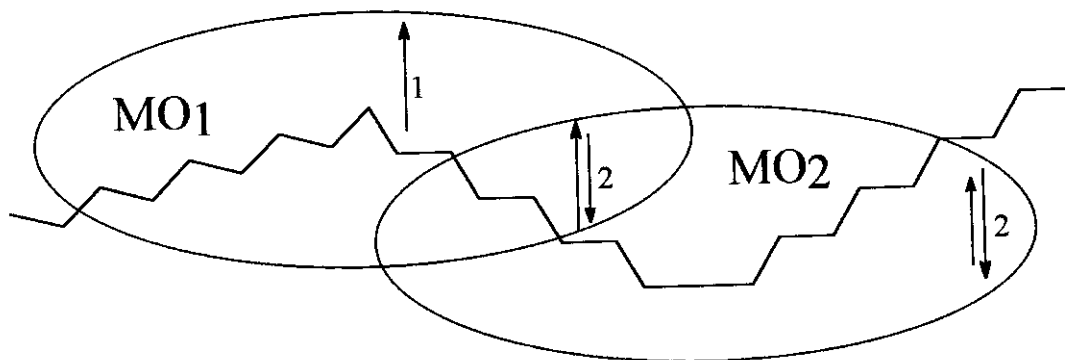


Figure 3. A molecular orbital  $MO_1$  containing an unpaired electron can spin-polarize another fully occupied molecular orbital  $MO_2$ . According to Hund's rule, in the region of overlap between the two orbitals, there will be a slight excess of  $MO_2$  spin population parallel to the unpaired spin in  $MO_1$ , while excess of antiparalle spin population will be present outside this region. Nuclei of atoms in the outer region of  $MO_2$  contributing to it with s-type orbitals will thus experience a

MO<sub>1</sub>. Unpaired spin density gets in contact with nuclei only through *s*-type orbitals, because they are the only orbitals with a finite electron density at the nucleus. The contact coupling constant, *A*, is related to the total unpaired spin density on a nucleus,  $\rho$ , through the following equation<sup>9,10</sup>:

$$A = \frac{\mu_0}{3S} \hbar \gamma_I g_e \mu_B \rho \quad (6)$$

where  $\mu_0$  is the magnetic permeability of a vacuum,  $\hbar$  is the Planck's constant,  $\gamma_I$  is the nuclear magnetogyric ratio and the other symbols have been already defined.

In the case of a single *S* manifold unsplit at zero field the contact shift is given by<sup>8,11</sup>:

$$\delta^{con} = -\frac{A}{\hbar \gamma_I B_0} \langle S_z \rangle = \frac{A}{\hbar} \frac{g_e \mu_B S(S+1)}{3 \gamma_I kT} \quad (7)$$

where  $\langle S_z \rangle$  is the expectation value of the  $S_z$  operator on an *S* multiplet, and is bound to the different population of the  $M_S$  levels, *k* is Boltzmann's constant, *T* the absolute temperature, and the other symbols have been already defined. This formula represents an approximation in the presence of large ZFS or other populated *S* multiplets.

The contact shift depends on the orientation of the molecule in the magnetic field if *g* is anisotropic and different from  $g_e$ . In solution the contact shift is an average given by **Equation 7** with an average value  $g_{av}$ .

The dipolar shift is provided by the magnetic field generated by the electron:

$$\delta^{dip} = \frac{1}{4\pi} \frac{1}{r^3} \chi (\frac{2}{3} \cos^2 \gamma - 1) \quad (8)$$

where *r* is the nucleus-electron distance (assuming the electron spin can be treated as a point dipole) and  $\gamma$  is the angle between the electron-nucleus vector and the direction of the magnetic field.

This formula assumes that all the unpaired electrons are localized on the metal ion. In principle, the integral should be made of the dipolar shift for each space volume where spin density occurs. Sometimes, the calculations are made assuming that ca. 60% of the electron is localized on

the metal and ca. 40% on the donor atoms, plus 1-2% of spin density on the various orbitals of other atoms of the donor groups. Such calculations provide the same results as in the MC case if a nucleus is more than 10 Å away from the metal and more than 3 Å away from an orbital bearing any spin density. This situation is common in proteins.

Upon rotation, the  $3\cos^2\theta-1$  term vanishes, and  $\delta^{dip}$  should be equal zero. However, if  $\chi$  is anisotropic the Zeeman energy changes with orientation and so does the excess population of a Zeeman level and therefore the spin density and the associated magnetic. Under these circumstances there is a shift, called pseudocontact shift (PCS), which, in the approximation that all the unpaired electrons are localized on the metal ion, is given by: <sup>11</sup>

$$\delta_{av}^{dip} = \delta^{pc} = \frac{1}{24\pi} \frac{1}{r^3} \left\{ \left[ 2\chi_{zz} - (\chi_{xx} + \chi_{yy}) \right] (3\cos^2\theta - 1) + 3(\chi_{xx} - \chi_{yy}) \sin^2\theta \cos 2\theta \right\} \quad (9)$$

where  $r$ ,  $\theta$  and  $\Omega$  are the polar coordinates of the nucleus in the reference frame of the tensor centered on the metal.

When the following relation holds

$$\chi = \mu_0 \mu_B^2 g_e^2 \frac{S(S+1)}{3kT}$$

the pseudocontact shifts can be expressed through the  $g$  tensor <sup>12</sup>:

$$\delta^{pc} = \frac{\mu_0}{4\pi} \frac{\mu_B^2 S(S+1)}{18kT} \frac{1}{r^3} \left\{ \left[ 2g_{zz}^2 - (g_{xx}^2 + g_{yy}^2) \right] (3\cos^2\theta - 1) + 3(g_{xx}^2 - g_{yy}^2) \sin^2\theta \cos 2\theta \right\} \quad (10)$$

These formulas apply to metal centered pseudocontact shifts (MCPCS). Let us now evaluate the contribution of spin density delocalization to PCS, called ligand centered PCS, abbreviated as LCPCS. The MO containing the unpaired electron has only one set of  $g$  values with its own orientations. Let us say that spin density is present in a  $p_\pi$  orbital of an  $sp^2$  carbon or nitrogen. The experimental value of  $\langle r^3 \rangle$  is  $3.2 \times 10^5 \text{ pm}^3$  for the heteronucleus and  $1.9 \times 10^6 \text{ pm}^3$  for an attached

proton<sup>13,14</sup>. With a metal-proton distance of 5 Å, a metal-heteronucleus distance of 4 Å,  $\theta = 0$  (maximum value) and 1% spin density on the  $p_\pi$  orbital the LCPCS is 200% and 60% of the MCPCS for the heteronucleus and the attached proton, respectively. This is an upper limit case, as spin polarization involves other orbitals with different  $g$  values whose evaluation has never been performed.

## 2.2. Nuclear relaxation

Nuclear relaxation rate enhancements occur whenever there are unpaired electrons. Unpaired electrons generate magnetic fields that are sensed by nuclei through the contact and dipolar mechanisms described in 2.1. As discussed in 1.1., fluctuations of these fields in time, with time constant  $\tau_c$ , cause nuclear relaxation. The rate enhancements due to contact mechanisms<sup>7,15,16</sup>, again in the approximation of a single  $S$  populated and unsplit at zero field for the longitudinal ( $R_1$ ), transverse ( $R_2$ ) and rotating frame ( $R_{1\rho}$ ) are:

$$R_{1M}^{con} = \frac{2}{3} S(S+1) \frac{A^2}{\hbar} \frac{\tau_c}{1 + \omega_s^2 \tau_c^2} \quad (11)$$

$$R_{2M}^{con} = \frac{1}{3} S(S+1) \frac{A^2}{\hbar} \frac{\tau_c}{1 + \omega_s^2 \tau_c^2} + \tau_c \quad (12)$$

$$q R_{1\rho M}^{con} = \frac{1}{3} S(S+1) \frac{A^2}{\hbar} \frac{\tau_c}{1 + \omega_s^2 \tau_c^2} + \frac{\tau_c}{1 + \omega_1^2 \tau_c^2} \quad (13)$$

where  $\omega_1$  is the nuclear Larmor frequency in the rotating frame and the other symbols have been already defined. Note that it is the magnetic moment of the entire electron which causes relaxation and not just the induced magnetic moment due to the excess spin population in the magnetic field. The correlation time  $\tau_c$  reflects the two types of fluctuations of the electron magnetic field at the nucleus, *i.e.* the fluctuation induced by electron relaxation, that changes the orientation of either the  $z$  or the  $xy$  components of the electron magnetic moment, or the fluctuation induced by interruptions of magnetic coupling due to chemical exchange, if present:

$$\tau_c^{-1}(con) = \tau_s^{-1} + \tau_M^{-1} \quad (14)$$

where  $\tau_s$  is the electronic correlation time and  $\tau_M$  is the time constant for chemical exchange.

The description of dipolar relaxation can be complicated, as for the dipolar shift, by delocalization of the electron. In the point dipole metal centered approximation, the relaxation enhancements are: <sup>7,16-18</sup>

$$R_{1M}^{dip} = \frac{2}{15} \frac{\mu_0}{4\pi} \frac{\gamma_I^2 g_e^2 \mu_B^2 S(S+1)}{r^6} \frac{7\tau_c}{1 + \omega_s^2 \tau_c^2} + \frac{3\tau_c}{1 + \omega_I^2 \tau_c^2} \quad (15)$$

$$R_{2M}^{dip} = \frac{1}{15} \frac{\mu_0}{4\pi} \frac{\gamma_I^2 g_e^2 \mu_B^2 S(S+1)}{r^6} \frac{13\tau_c}{1 + \omega_s^2 \tau_c^2} + \frac{3\tau_c}{1 + \omega_I^2 \tau_c^2} + 4\tau_c \quad (16)$$

$$R_{1\rho M}^{dip} = \frac{1}{15} \frac{\mu_0}{4\pi} \frac{\gamma_I^2 g_e^2 \mu_B^2 S(S+1)}{r^6} \frac{13\tau_c}{1 + \omega_s^2 \tau_c^2} + \frac{3\tau_c}{1 + \omega_I^2 \tau_c^2} + \frac{4\tau_c}{1 + \omega_1^2 \tau_c^2} \quad (17)$$

Here  $\tau_c$  is given by:

$$\tau_c^{-1}(dip) = \tau_s^{-1} + \tau_M^{-1} + \tau_r^{-1} \quad (18)$$

because, when the electron and nuclear spins do not coincide in space, rotation ( $\tau_r$ ), besides electron relaxation ( $\tau_c$ ) and chemical exchange ( $\tau_M$ ), is also a mechanism to modulate the electron magnetic field at the nucleus. In the case of lanthanides the total - orbital plus spin - magnetic moment,  $J$ , should substitute  $S$ . The metal centered dipolar approximation has been found to be satisfactory except when a nucleus experiences some spin density on a  $p$  orbital or when a proton is attached to an atom carrying spin density on a  $p$  orbital.

When  $S > 1$ , there are more than one electronic relaxation times which should be used in predicting nuclear relaxation <sup>4</sup>. Further comments are given in Section 4.

The induced magnetic moment which is due to the different population of the Zeeman levels and causes the hyperfine shift also causes relaxation. This magnetic moment is a small fraction of

magnetic fields and long rotational correlation times, the dipolar coupling may provide large nuclear relaxation enhancements, particularly of  $R_2$  and  $R_{1\rho}$ <sup>19-21</sup>:

$$R_{1M}^{Cur} = \frac{2}{5} \frac{\mu_0}{4\pi} \frac{\omega_I^2 g_e^4 \mu_B^4 S^2 (S+1)^2}{(3kT)^2 r^6} \frac{3\tau_c}{1 + \omega_I^2 \tau_c^2} \quad (19)$$

$$R_{2M}^{Cur} = \frac{1}{5} \frac{\mu_0}{4\pi} \frac{\omega_I^2 g_e^4 \mu_B^4 S^2 (S+1)^2}{(3kT)^2 r^6} \frac{3\tau_c}{1 + \omega_I^2 \tau_c^2} + 4\tau_c \quad (20)$$

$$R_{2M}^{Cur} = \frac{1}{5} \frac{\mu_0}{4\pi} \frac{\omega_I^2 g_e^4 \mu_B^4 S^2 (S+1)^2}{(3kT)^2 r^6} \frac{3\tau_c}{1 + \omega_I^2 \tau_c^2} + \frac{4\tau_c}{1 + \omega_I^2 \tau_c^2} \quad (21)$$

Here  $\tau_c$  is given by:

$$\tau_c^{-1}(Cur) = \tau_M^{-1} + \tau_r^{-1} \quad (22)$$

These mechanisms are referred to as Curie relaxation mechanisms because they are concerned with the excess spin along  $B_0$ . Note that whereas the previously described contributions to  $R_2$  and  $R_{1\rho}$  decrease with increasing magnetic field to a plateau, the present dipolar mechanism increases with the square of the magnetic field and represents a serious limitation to high field investigations of paramagnetic metalloproteins. The Curie contribution to  $R_1$  is less important. The contribution to contact relaxation is also minor because rotation cannot modulate the interaction between two magnetic dipoles starting from the same point and aligned along the external magnetic field. Only chemical exchange can modulate such interaction.

Ligand-centered dipolar relaxation mechanisms can be operative and effective in the case of an  $sp^2$  heteroatom and its attached proton if spin density is present on its  $p_z$  orbital<sup>13,14</sup>.

### 3. Gains and losses from the NMR viewpoint

For high resolution NMR the presence of unpaired electrons is a limitation which may be more or less severe. At the same time precious information may be obtained on the hyperfine

coupling of the type ENDOR spectroscopists obtain; finally, unique information on the time modulation of the hyperfine coupling may be gained.

The general attitude of the high resolution NMR spectroscopists dealing with paramagnetic molecules is that of trying to minimize the effects on nuclear  $R_1$ ,  $R_2$  and  $R_{1\rho}$  and to overcome the effects of fast relaxation which reduce the detectability of scalar and dipolar nucleus-nucleus interactions. In favorable cases the loss of connectivities is limited and is more than compensated by the information contained in the analysis of the hyperfine coupling effects. In unfavorable cases the lines are so much broadened that signals escape detection. In these cases, however, we may exploit fast exchange with excess ligand nuclei to detect the signal. Under these circumstances we learn more on the modulation of the hyperfine coupling than when the linewidth is only moderately broadened.

In proteins the correlation time for nuclear relaxation is almost always determined by  $\tau_s$  since rotation is slow and exchange, if present, is also slower than  $\tau_s$ . The  $\tau_s$  values for many common metal ions are reported in **Table 1** together with the proton linewidth due to dipolar relaxation ( $\pi\Delta\nu = R_2$ ) at a distance of 5 Å at 500 MHz. Along this chapter we define  $10^{-11}$  s as the approximate borderline for  $\tau_s$ : when  $\tau_s$  is shorter, high resolution NMR can be attempted; when  $\tau_s$  is longer one should exploit nuclear relaxation at its best. Of course, for the largest S values even shorter  $\tau_s$  values are necessary to obtain high resolution spectra, whereas for the smallest S value high resolution spectra are obtained also for somewhat larger  $\tau_s$  values (**Figure 4**).

Table 1.  $\tau_S$  values for common metal ions and their consequences on nuclear relaxation rates,  $R_{1,2M}$ .<sup>a</sup> (adapted from <sup>38,100</sup>).

Paramagnetic system	$S$	$\tau_S$ (s <sup>-1</sup> )	small molecules ( $\tau_r = 10^{-10}$ s <sup>-1</sup> ) $R_{1,2M}^I$	large molecules ( $\tau_r = 10^{-8}$ s <sup>-1</sup> ) $R_{1M}^I$ $R_{2M}^I$	
organic radicals	1/2	$10^{-6}$ - $10^{-8}$	300-500	10-40	15000-30000
Ti <sup>3+</sup>	1/2	$10^{-10}$ - $10^{-11}$	40-300	40-400	100-500
VO <sup>2+</sup>	1/2	$10^{-8}$	300-500	30	15000
V <sup>3+</sup>	1	$10^{-11}$	100-150	100	500
V <sup>2+</sup>	3/2	$10^{-9}$	1500-2000	1000	15000
Cr <sup>3+</sup>	3/2	$5 \times 10^{-9}$ - $5 \times 10^{-10}$	1500-2000	200-1500	10000-60000
Cr <sup>2+</sup>	2	$10^{-11}$ - $10^{-12}$	50-500	40-400	4000
Mn <sup>3+</sup>	2	$10^{-10}$ - $10^{-11}$	300-2000	300-3000	4000-8000
Mn <sup>2+</sup>	5/2	$10^{-8}$	4000-6000	400	200000
Fe <sup>3+</sup> (H.S.)	5/2	$10^{-9}$ - $10^{-11}$	500-6000	500-3000	8000-50000
Fe <sup>3+</sup> (L.S.)	1/2	$10^{-11}$ - $10^{-13}$	2-50	1-60	50-150
Fe <sup>2+</sup> (H.S.)	2	$10^{-12}$ - $10^{-13}$	50-150	10-50	4000
Co <sup>2+</sup> (H.S., 5-6 <sub>coord</sub> )	3/2	$5 \times 10^{-12}$ - $10^{-13}$	20-200	10-2000	1000-2000
Co <sup>2+</sup> (H.S., 4 <sub>coord</sub> )	3/2	$10^{-11}$	200-300	200	2000
Co <sup>2+</sup> (L.S.)	1/2	$10^{-9}$ - $10^{-10}$	200-400	200-400	500-3000
Ni <sup>2+</sup> (5-6 <sub>coord</sub> )	1	$10^{-12}$	600-700	1000	2000
Ni <sup>2+</sup> (4 <sub>coord</sub> )	1	$10^{-10}$	20-30	20	400
Cu <sup>2+</sup>	1/2	$10^{-9}$	300-500	40-200	3000-20000
Ru <sup>3+</sup>	1/2	$10^{-11}$ - $10^{-12}$	5-50	5-50	50-150
Re <sup>3+</sup>	2	$10^{-12}$ - $10^{-13}$	50-150	10-50	4000
Gd <sup>3+</sup>	7/2	$10^{-8}$ - $10^{-9}$	5000-15000	800-5000	100000-400000
<b>J</b>					
Ce <sup>3+</sup>	5/2	$10^{-13}$	7-8	4	300
Pr <sup>3+</sup>	4	$3 \times 10^{-13}$ - $6 \times 10^{-14}$	16-30	5-13	1000
Nd <sup>3+</sup>	9/2	$2 \times 10^{-13}$	20-30	10	1100
Sm <sup>3+</sup>	5/2	$2 \times 10^{-13}$ - $5 \times 10^{-14}$	0.2-0.6	0.2-0.5	3-4
Eu <sup>2+</sup>	7/2	$10^{-14}$	300-400	20	30000
Tb <sup>3+</sup>	6	$2 \times 10^{-13}$	800-1000	120	60000
Dy <sup>3+</sup>	15/2	$1 \times 10^{-12}$ - $4 \times 10^{-13}$	1100-1500	170-300	80000
Ho <sup>3+</sup>	8	$1 \times 10^{-13}$ - $2 \times 10^{-13}$	1100-1500	150-200	80000

Er <sup>3+</sup>	15/2	8x10 <sup>-13</sup> -3x10 <sup>-13</sup>	700-1000	120-200	50000
Tm <sup>3+</sup>	6	5x10 <sup>-13</sup>	300-400	80	20000
Yb <sup>3+</sup>	7/2	5x10 <sup>-13</sup> -2x10 <sup>-13</sup>	50-70	16-30	3000

<sup>a</sup>. Calculated at 298 K, 800 MHz proton Larmor frequency, 5 Å electron-nucleus distance, including Curie relaxation. Organic radicals are reported for comparison purposes.

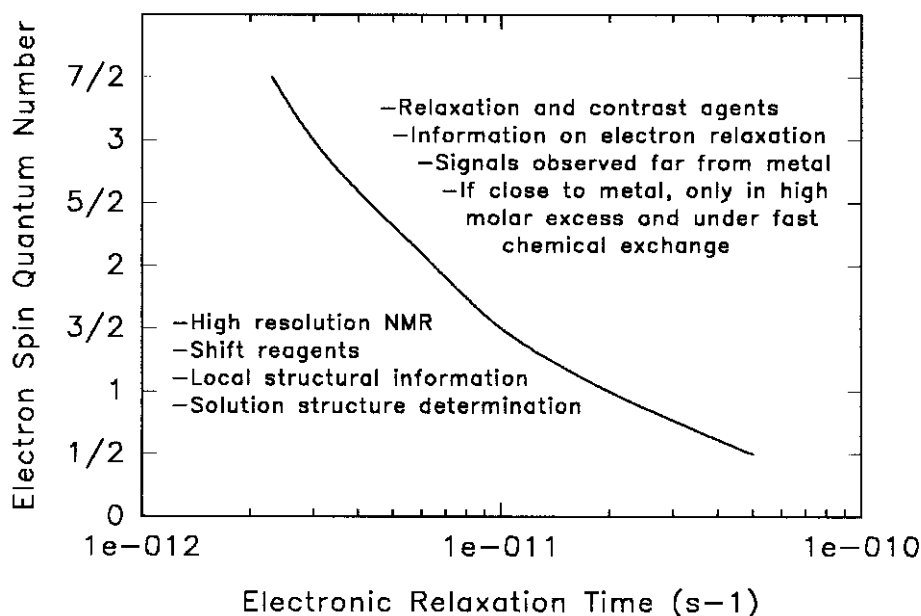


Figure 4. Information obtained from NMR of paramagnetic systems under weak (lower left) and strong (upper right) nuclear relaxing ability. The nuclear relaxing ability increases with increasing electron spin quantum number and with increasing electronic relaxation time. A nuclear relaxing ability that induces a dipolar line broadening of about 300 Hz for a proton at 4 Å from the metal is taken as the borderline case.

Ideally, a sample should give rise to large hyperfine shifts (contact + pseudocontact) and to small broadening. This provides information on the hyperfine coupling energy and makes the assignment accessible. In the case of metalloproteins, hyperfine shifted signals easily fall outside the range of diamagnetic signals. This happens when lanthanides and some cobalt(II) (in general with coordination number larger than 4) or low spin iron(III) ions constitute the paramagnetic center (see Chapter 10). Generally, metal ions with short  $\tau_s$  have low-lying excited levels and strong spin orbit coupling effects which cause magnetic susceptibility anisotropy and then pseudocontact shifts. In magnetic coupled systems containing two or more metal ions there is only a  $\tau_s$  if the

magnetic coupling energy divided by  $\hbar$  is larger than  $\tau_s^{-1}$  of each separated metal ion. In these cases often  $\tau_s$  is small (see later). So, the shifts, and particularly contact shifts, can be large and the line broadening modest.

In the cases of manganese(II) and gadolinium(III) the broadening is larger than the shift (see Section 4.), and signals may be broadened beyond detection before they are shifted *e.g.* outside the diamagnetic part of the protein. In between the above limits there are other cases for which the hyperfine shifted signals are well spread but suffer of sizable line broadening.

Dipolar line broadening and longitudinal relaxation depends on  $r^{-6}$ , the reciprocal of the sixth power of the metal-nucleus distance, and on  $\tau_s$ . The longer  $\tau_s$ , the farther away from the metal ion is the window of observation of broadening. For  $\text{Mn}^{2+}$  broadening can be observed 25 Å away. On the other limit, when  $\tau_s$  is short, no hyperfine broadening is observed 10 Å away. The decay of paramagnetic dipolar  $R_1$  and  $R_2$  enhancements for  $^1\text{H}$ ,  $^{13}\text{C}$  and  $^{15}\text{N}$  nuclei in metalloproteins are reported in **Figure 5** as a function of the distance from the metal ion. Note that the effect on heteronuclei is much smaller due to their smaller magnetogyric ratio.

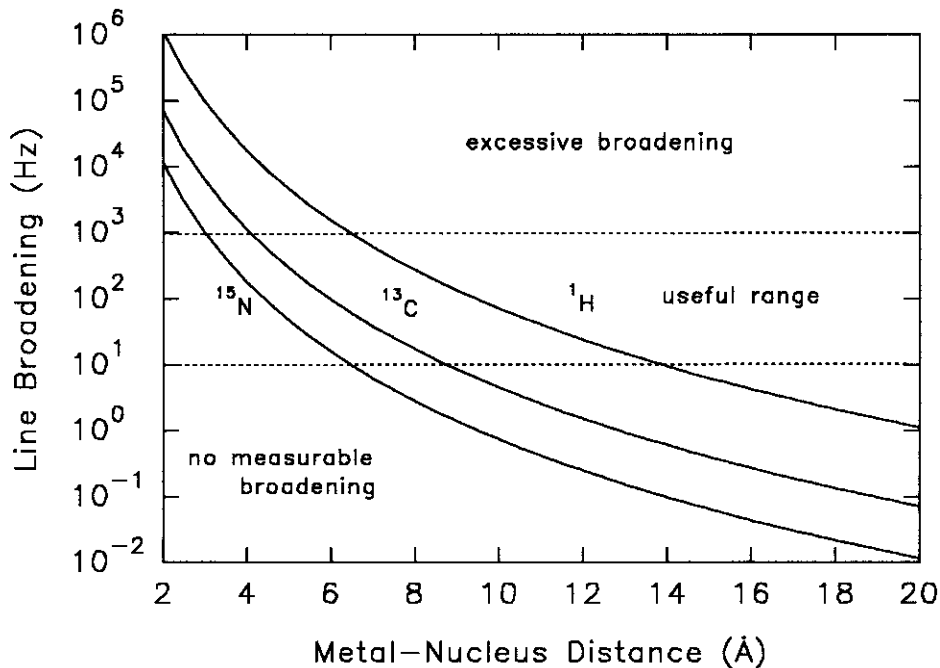


Figure 5. Differential line broadening effects of a paramagnetic center on different nuclei. The useful linewidth range for obtaining structural information is shown. The curves are calculated for dipolar and Curie relaxation induced at 500 MHz proton Larmor frequency by an  $S = 5/2$  ion with  $\tau_s = 2 \times 10^{-10}$  s in a molecule with  $\tau_r = 10^{-8}$  s.

When  $\tau_s$  is short, nuclear longitudinal relaxation is moderately affected and NOEs between protons can be easily measured. NOEs depend on longitudinal relaxation (see Chapter 5) of the connected nuclei. The same holds for scalar coupling detection, which depends on  $R_2$ . As already mentioned, heteronuclei are less severely affected by paramagnetism owing to their low magnetogyric ratio, and  $^1J$  values between heteronuclei and protons are at least one order of magnitude larger than proton-proton  $^nJ$  values. Therefore, hetero-correlation experiments are successfully performed as long as the proton lines are not too severely broadened. For example,  $^1\text{H}$ - $^{15}\text{N}$  HSQC (see...) experiments allow the detection of crosspeaks when the proton lines are as large as 250 Hz (signals B and K in **Figure 6**)<sup>22</sup> whereas no HSQC cross peak could be detected for the 500 Hz broad signal C. Concluding, structural information can be derived from high resolution NMR. Furthermore, pseudocontact shifts and nuclear relaxation can be used for structural information (see Chapter 10).

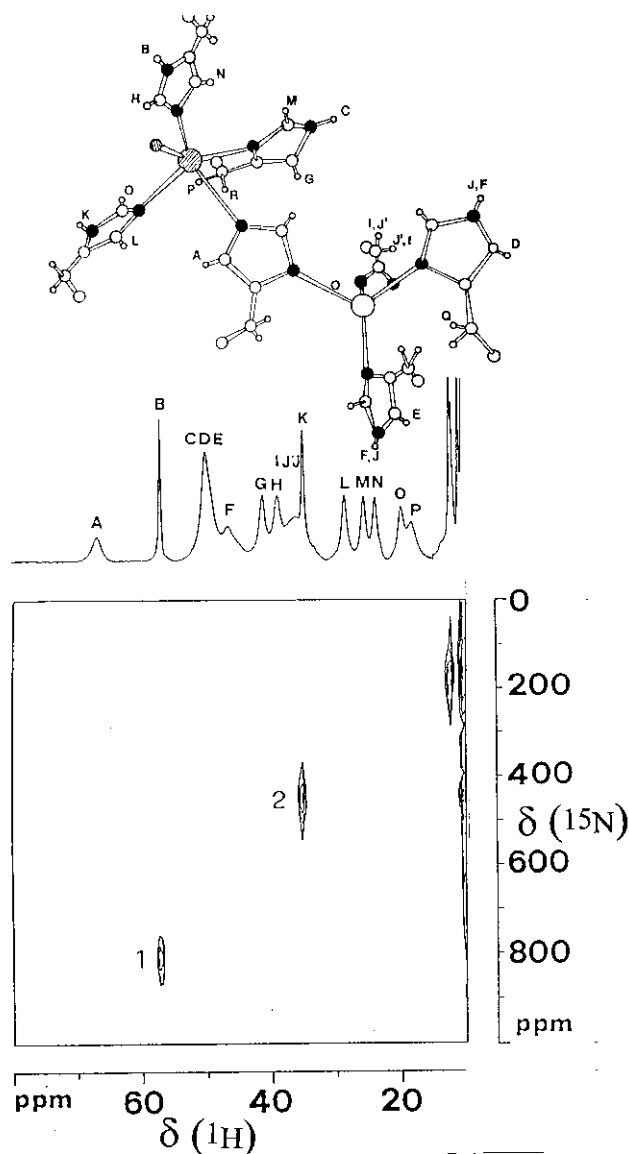


Figure 6. 600 MHz <sup>1</sup>H-<sup>15</sup>N HMQC spectrum of Cu<sub>2</sub>Co<sub>2</sub>SOD. The active site scheme with the proton assignment is also shown (Cu = shaded sphere, Co = hollow sphere). The cross-peaks refer to distal NHs of copper-coordinated histidines, B and K. The experiment used a four-pulse scheme<sup>110</sup> with the delay between the first two pulses matching the reciprocal of the proton linewidths<sup>22</sup>.

As it will be shown below, systems with short  $\tau_s$  are such that  $\omega^2\tau_s^2 \ll 1$  for accessible magnetic fields and the information on electron relaxation is modest. When on the contrary  $\tau_s$  is long, under the conditions of signal detection a lot can be learned on the electron spin energy and dynamics.

#### 4. Solvent relaxometry

Several paramagnetic metalloproteins have one or more water molecules coordinated to the metal ion which are in exchange with the bulk solvent. The measurements of relaxation of solvent nuclei at various magnetic fields was soon<sup>23,24</sup> recognized to potentially provide a wealth of information. However, few chemists were attracted by the field, which tended to become more popular with the application of contrast agents in MRI (see later). The Florence laboratory exploited this technique to understand electron relaxation in solution, which is fundamental for NMR spectroscopy. Therefore, together with a few other groups, like Kowalewski's, theoretical tools based on the spin Hamiltonian were developed to interpret the experimental data<sup>25-31</sup>.

The water proton longitudinal relaxation is given by:

$$R_1 = R_{1dia} + R_{1p} \quad (23)$$

where  $R_1$  is the experimental value,  $R_{1dia}$  is the diamagnetic contribution and  $R_{1p}$  is the paramagnetic contribution.  $R_{1dia}$  can be determined using the apoprotein or a diamagnetic metal, *e.g.*  $Zn^{2+}$ . In turn<sup>32</sup>,

$$R_{1p} = [f (T_{1M} + \tau_M)]^{-1} \quad (24)$$

where  $f$  is the molar fraction of solvent bound to the metal,  $\tau_M$  is the exchange time and  $T_{1M} = R_{1M}^{-1}$  is the relaxation time of the protons of the solvent molecules bound to the metal ion. If the exchange time  $\tau_M$  is long with respect to  $T_{1M}$  its reciprocal determines  $R_{1p}$ . The paramagnetic effect is small and is generally revealed through variable temperature measurements since the exchange rate increases with increasing temperature with an Arrhenius type law:

$$\tau_M^{-1} = \frac{kT}{h} \exp \frac{-G}{RT} \quad (25)$$

where  $\Delta G^\ddagger$  is the free energy of activation for the exchange process and  $R = kN_A$  where  $N_A$  is Avogadro's constant. When  $\tau_M$  is negligible with respect to  $T_{1M}$ , then

$$R_{1p} = (fT_{1M})^{-1} \quad (26)$$

and  $T_{1M}$  is easily determined. Apparatuses, called relaxometers, to measure water  $^1\text{H}$   $T_1$  between 0.01 or 0.001 MHz to a few tens of MHz are nowadays available. By using standard spectrometers, the relaxometry measurements can be extended to 800 MHz. In the case of water, MC dipolar relaxation is the main longitudinal relaxation mechanism<sup>33</sup>. A relaxometry profile calculated according to **Equation 15** is reported in **Figure 7**.

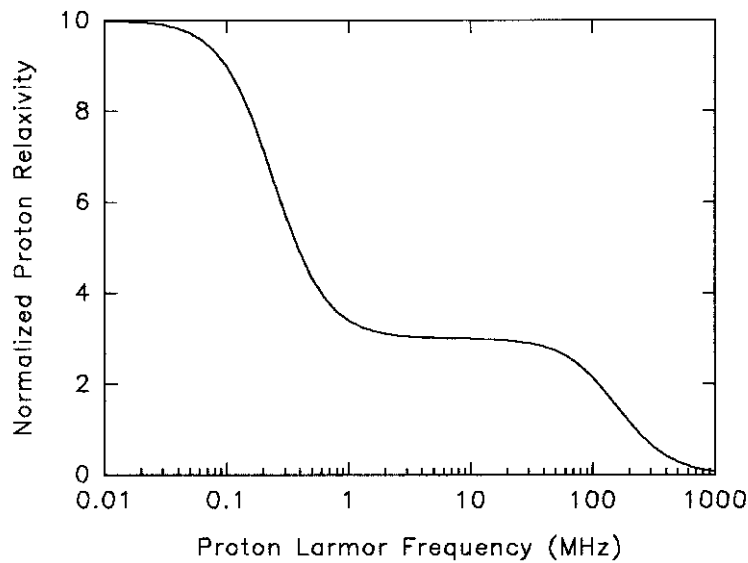


Figure 7. Normalized  $^1\text{H}$  relaxometry profile calculated according to Equation 15 with  $\tau_c = 10^{-9}$  s.

If  $R_{1M}$  at low fields is taken equal to 10, there is a dispersion with inflection at  $\omega_s\tau_c = 1$ , then a plateau with a  $R_{1M}$  value of 3, and eventually another dispersion at  $\omega_l\tau_c = 1$  which brings  $R_{1M}$  to zero. Indeed, the experimental profiles may look very different because at low magnetic field the  $S$  manifold is split by terms of the spin Hamiltonian of the type

$$H = I_M A S \quad (27)$$

where  $I_M$  is the metal nuclear spin operator and the term refers to the splitting of the  $S$  manifold by coupling with the metal nucleus<sup>34</sup>, and

$$H = S D S \quad (28)$$

where  $D$  is the ZFS parameter and the term refers to the splitting of the  $S$  manifold due to spin orbit coupling<sup>28-30,35,36</sup>. The effects of these terms on relaxometry profiles have been worked out and a general computer program that takes them into account is available<sup>25</sup>.

The above effects become important when  $\hbar\tau_c^{-1} \ll A, D$ . In aqua complexes  $\tau_r$  is of the order of 30-100 ps<sup>37</sup>. Information on  $\tau_s$  is available if  $\tau_s$  is shorter than the above values. However, if  $\tau_s$  is much shorter than 30 ps, the  $\omega_s\tau_s = 1$  dispersion occurs at proton Larmor frequencies higher than 10 MHz, and the  $\omega_r\tau_s = 1$  dispersion occurs at proton Larmor frequencies 658 times higher! Under such circumstances little information is available from variable magnetic field studies. Finally, it is common that for short  $\tau_s$  (and  $\tau_c$ ) the splitting of the  $S$  manifold is small with respect to the energy uncertainty (*i.e.*  $\hbar\tau_c^{-1} \gg A, D$ ). When  $\tau_s$  is larger than  $10^{-10}$  s,  $\tau_r$  determines the correlation time of small metal complexes. Viscous solvents like ethyleneglycol or glycerol can be used to increase  $\tau_r$  and to make  $\tau_s$  the correlation time for nuclear relaxation<sup>38-42</sup>. In metalloproteins  $\tau_r$  is  $10^{-8}$  s, and  $\tau_s$  is the correlation time. Since  $\tau_s$  cannot be shorter than the correlation time ( $\tau_v$ ) relative to the mechanisms which cause electron relaxation, when  $\tau_s$  is shorter than  $10^{-11}$  s (*e.g.*  $10^{-12}$  s), then reference should be made to solid state electron relaxation mechanisms which occur on the vibrational time scale ( $10^{-13}$  s). In the cases of long  $\tau_s$ , the correlation times  $\tau_v$  may be related to molecular movements. In solution the solvent collisions can be a mechanism which causes electron relaxation<sup>43,44</sup>. Its correlation time can be the solvent diffusion which is a few picoseconds. When the interaction between the metal ion and colliding molecules is mediated by the protein part, such correlation time may increase up to one order of magnitude<sup>38,45,46</sup>. An equation is available which relates the electronic relaxation times  $R_{1e}$  and  $R_{2e}$  with the colliding time and the induced dynamic ZFS<sup>4,43</sup>:

$$R_{1e} = \frac{2}{50} [4S(S+1) - 3] \frac{\tau_v}{1 + \omega_s^2 \tau_v^2} + \frac{4\tau_v}{1 + 4\omega_s^2 \tau_v^2} \quad (29)$$

$$R_{2e} = \frac{2}{50} [4S(S+1) - 3] 3\tau_v + \frac{5\tau_v}{1 + \omega_s^2 \tau_v^2} + \frac{2\tau_v}{1 + 4\omega_s^2 \tau_v^2} \quad (30)$$

where  $\Delta$  is the amplitude of the dynamic ZFS induced by collisions. Something similar may hold for the modulation of the hyperfine coupling between the metal nucleus and the unpaired electron<sup>47-49</sup>. In **Table 2** the electronic relaxation times of some metal water complexes and the electronic relaxation mechanisms are reported. **Equation 29** predicts that when there is a  $\tau_v$  dispersion,  $R_{1e}^{-1} = \tau_s$  increases and so does  $R_{1M}$  (**Figure 8**). This happens until  $\tau_s^{-1}$  reaches  $\tau_r^{-1}$  or  $\tau_M^{-1}$  and then the  $\omega\tau_c = 1$  dispersion takes over and  $R_{1M}$  decreases again. A bell-type nuclear relaxation behavior is expected and indeed found as shown in **Figure 8**. This behavior is shown by macromolecular systems containing  $Mn^{2+}$ <sup>38,45,46</sup> or  $Gd^{3+}$ <sup>38,42,46,50</sup>. The latter ion is used as contrast agent in MRI (see Section 5.3.).

Table 2. Electronic relaxation times and relaxation mechanisms of some metal-water complexes.

aqua ion	$I$	$S$	$A/h$ (MHz)	$\tau_{s0}$ (ps) <sup>a</sup>	$\tau_v$ (ps)	$\tau_c$	relaxation mechanism <sup>a</sup>
$\text{Cu}(\text{OH}_2)_6^{2+}$	3/2	1/2	0-0.2	300	0	$\tau_r$	A, B, C
$\text{VO}(\text{OH}_2)_5^{2+}$	7/2	1/2	2.1	400	6	$\tau_r$	D
$\text{Ti}(\text{OH}_2)_6^{3+}$		1/2	4.5	40	0	$\tau_r - \tau_s$	B
$\text{Mn}(\text{OH}_2)_6^{2+}$	5/2	5/2	0.6-1.0	3500	5.3	$\tau_r$	E
$\text{Fe}(\text{OH}_2)_6^{3+}$		5/2	0.4-1.2	84	5.9	$\tau_r - \tau_s$	E
$\text{Fe}(\text{OH}_2)_6^{2+}$		2		1	0	$\tau_s$	B
$\text{Cr}(\text{OH}_2)_6^{3+}$		3/2	2.0	500	0	$\tau_r$	E
$\text{Co}(\text{OH}_2)_6^{2+}$	7/2	3/2	0.1	3-6	0	$\tau_s$	B
$\text{Ni}(\text{OH}_2)_6^{2+}$		1	0.2	3-10	2.2	$\tau_s$	E
$\text{Gd}(\text{OH}_2)_9^{3+}$		7/2	0	130	16	$\tau_r$	E
$\text{Ln}(\text{OH}_2)_9^{3+}$			0	1-0.1	0	$\tau_s$	B, F

<sup>a</sup> A: Raman; B: Orbach; C: spin-rotation; D: A-anisotropy; E: ZFS modulation; F: Curie <sup>38</sup>.

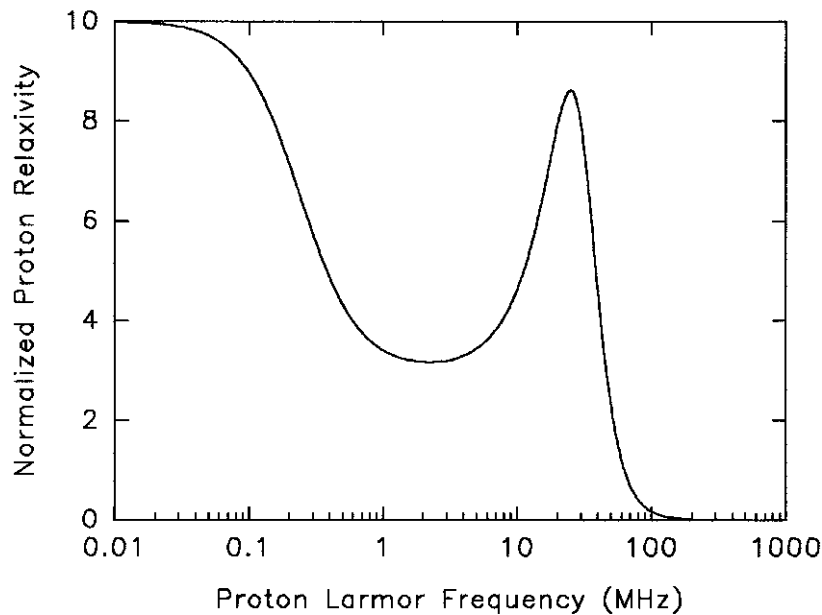


Figure 8. Normalized  $^1\text{H}$  relaxometry profile calculated according to Equation 15 with  $\tau_c = \tau_s = R_{1e}^{-1}$  from Equation 29, and  $S=7/2$ ,  $\Delta = 10^{10} \text{ s}^{-1}$  and  $\tau_v = 10^{-11} \text{ s}$ . Note the sharp increase in relaxivity above 10 MHz due to the increase in  $\tau_s$  from Equation 29 and the sharp decrease above 30 MHz due to the onset of the  $\omega_I$  dispersion in Equation 15.

As a complicated example the profile of iron(III) transferrin is reported in **Figure 9**<sup>51</sup>. At 0.1 MHz the  $\omega_s\tau_s=1$  dispersion is observed, at 5 MHz a small step is observed which is attributed to the electron Zeeman energy becoming equal to ZFS, then the  $\tau_v$  dependent nuclear relaxation enhancement occurs and finally the  $\omega_I\tau_c = 1$  dispersion begins. The parameters which simulate such curve are reported in the caption of **Figure 9**.

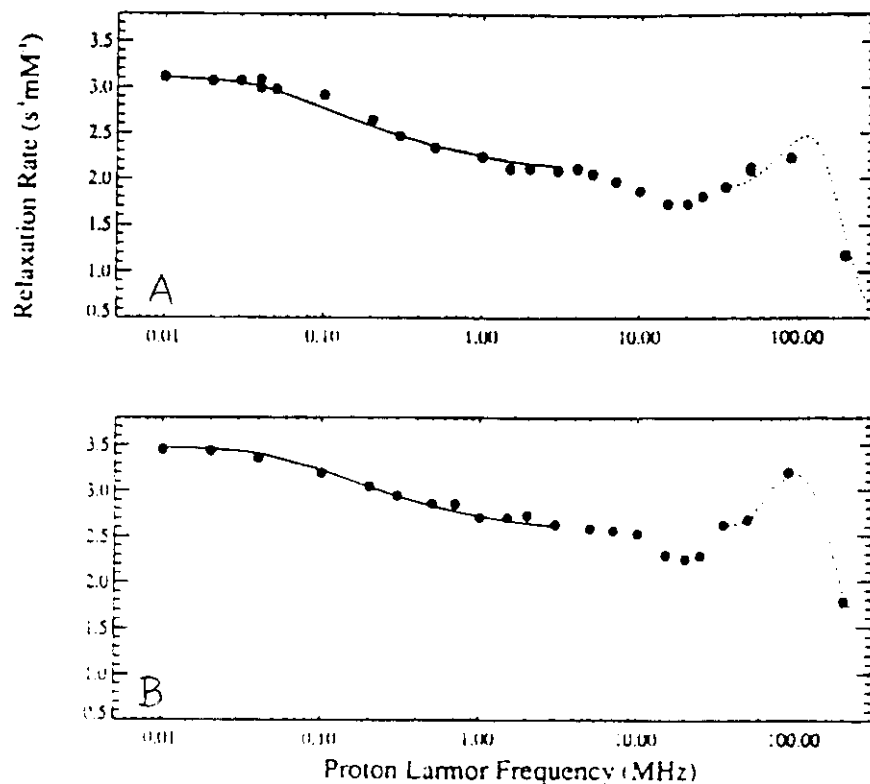


Figure 9. Relaxometry profiles of diferric transferrin solutions at 293 (A) and 308 K (B) <sup>51</sup>. The solid and dotted curves refer to separate fittings of the low and high field regions. The best fit parameters are:  $r_{MH} = 4 \text{ \AA}$ ,  $\Delta = 0.095 \text{ cm}^{-1}$ ,  $D = 0.2 \text{ cm}^{-1}$ ,  $E/D = 0.33$ ,  $\theta = 90^\circ$ ,  $\phi = 55^\circ$ ,  $\tau_x = 1.3 \text{ ns}$  (293 K) or 1.1 ns (308 K),  $\tau_y = \tau_z = 0.32 \text{ ns}$  (293 K) or 0.30 ns (308 K), where  $D$ ,  $E$ ,  $\theta$  and  $\phi$  are ZFS parameters and the  $\tau_s$  values are distinct according to the directions of the ZFS tensor.

Relaxometry is the NMR technique which allows us to estimate the electronic relaxation times of the various metal ions and to predict the broadening of the NMR signals. In Table 1 the broadening due to dipolar coupling of a proton at 5 Å distance from the metal ion at 800 MHz is reported. This table allows us to classify metal ions suitable for high resolution NMR because the line broadening is moderate, and those which broaden dramatically the NMR line and can be used as relaxation reagents.

## 5. Paramagnetic ions as probes

### 5.1. Shift reagents

Shift reagents are called those metal ions or their metal complexes which induce hyperfine shifts with tolerable line broadening when associated to a diamagnetic molecule. Typically, they are lanthanides(III) (except gadolinium(III)) and cobalt(II), the latter when 5- or 6-coordinated. Lanthanide complexes have been used since the sixties to increase the resolution of the NMR spectra of organic molecules<sup>52-54</sup>. **Figure 10** shows the spreading of the 60 MHz NMR signals of the CH<sub>2</sub> groups of hexylalcohol upon addition of the shift reagent Eu(FOD)<sub>3</sub><sup>52</sup>. Then shift reagents have been used with small molecules of biological relevance to learn about the structure of the molecules . and finally, for the same purpose, the metal ions alone have been used as substituents of calcium in calcium binding proteins (see Chapter 10).

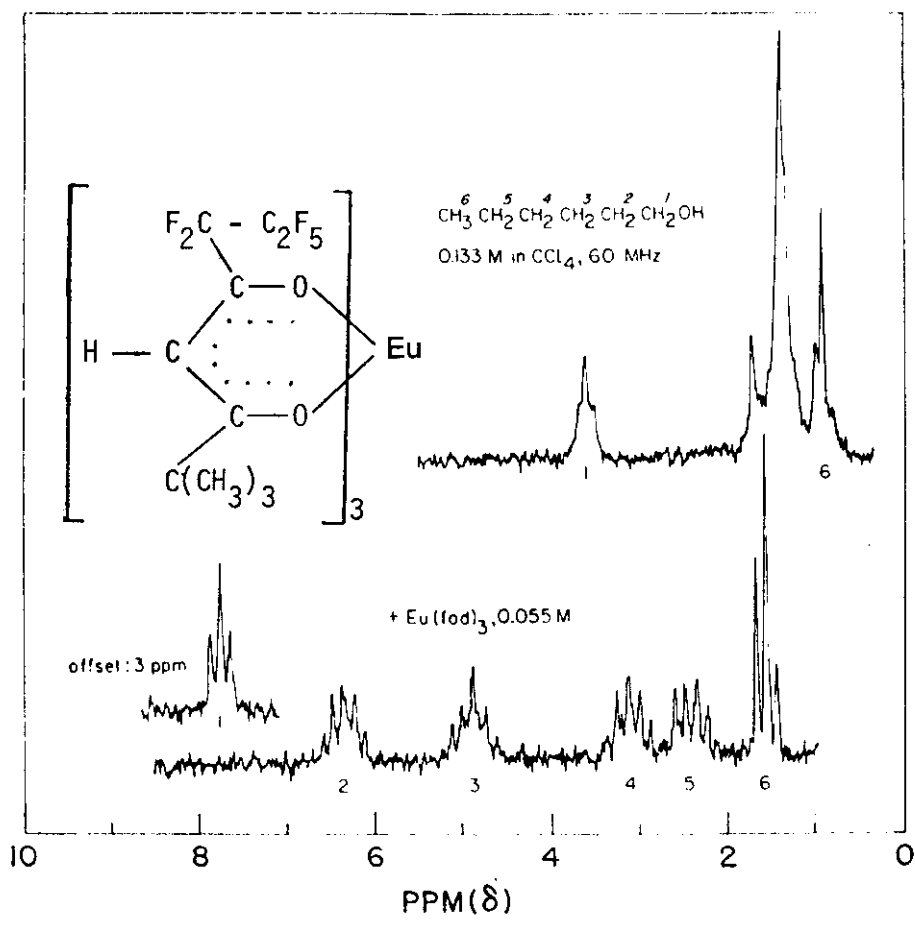


Figure 10. Historical 60 MHz <sup>1</sup>H NMR spectrum of 1-hexanol showing the increase in resolution obtained in the presence of Eu(FOD)<sub>3</sub> (inset). Methylene protons in positions 2 to 5 are unresolved, and become clearly resolved in the presence of the shift reagent<sup>52</sup>.

The use of shift reagents in organic chemistry has been largely abandoned with the availability of large magnetic fields and multi-dimensional NMR. The use of shift reagents to probe molecular structures through **Equation 9** for pseudocontact shifts is limited, as it is for NOEs<sup>55</sup>, by the possible existence of conformers which are in fast equilibrium on the NMR time scale and therefore may provide unrealistic coordinates for the resonating nuclei. The use of lanthanides in proteins has been shown to be promising. The first applications<sup>56</sup> suffered from the lack of 2D NMR techniques for signal assignment, which was very tentative and possibly only consistent with the net of pseudocontact shifts. Then 2D NMR was used for achieving firm assignments, which provided a  $\chi$  tensor and in turn generated calculated shifts for other nuclei whose assignment was subsequently confirmed by 2D spectroscopy<sup>57</sup>. This cyclic procedure has eventually led to the resolution of a 3D structure of a cerium(III) protein (see also Chapter 10)<sup>58</sup>. The limits here are that lanthanides with  $S > 1/2$  (or  $J > 1/2$ ) broaden beyond detection the lines of the directly coordinated groups due to Curie relaxation, that is proportional to the square of  $S(S + 1)$  or  $J(J + 1)$  (**Equation 20**) and with the  $S=1/2$  ion (cerium(III)) measurable pseudocontact shifts are only obtained from nuclei within a sphere of about 10 Å from the metal ion.

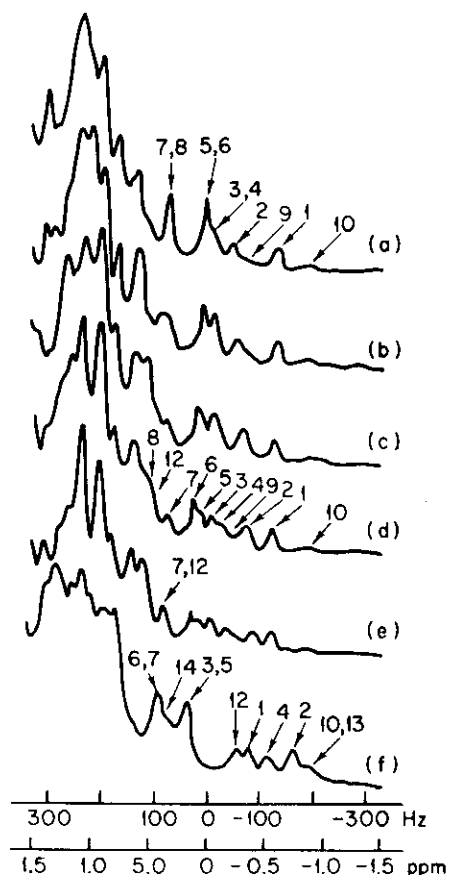


Figure 11. Historical  $^1\text{H}$  NMR titration of lysozyme (7 mM) with  $\text{Co}^{2+}$  (0, 1.75, 3.5, 7, 10.5, 155 mM from *a* to *f*). The labeled signals arise from aminoacid residues that selectively interact with the added  $\text{Co}^{2+}$  ions in fast exchange <sup>59</sup>.

Cobalt(II) has been used in early times to shift the resonances of lysozyme (**Figure 11**) <sup>59</sup> and to substitute zinc in several zinc proteins <sup>60</sup>. Typically, the substitution of cobalt(II) with zinc in carbonic anhydrase in the presence of anions which give rise to 5-coordinated derivatives has provided very sharp NMR signals shifted far away <sup>60-67</sup>. The signals of coordinated histidines could therefore be monitored (**Figure 12a**). It is instructive to observe that when the derivative is tetraordinated as in the case of the  $\text{NCO}^-$  derivative the shifts are smaller and the lines broader. Tetrahedral cobalt(II) has electronic relaxation times one order of magnitude larger than 5- or 6-coordinated cobalt(II) on account of the different electronic structure <sup>60,61,68-70</sup> and therefore we move from shift reagents to relaxation reagents (**Figure 12b**). Shift reagents in a modern sense are those metal ions with short  $\tau_s$ , for which high resolution NMR can be performed successfully (see Chapter 10).

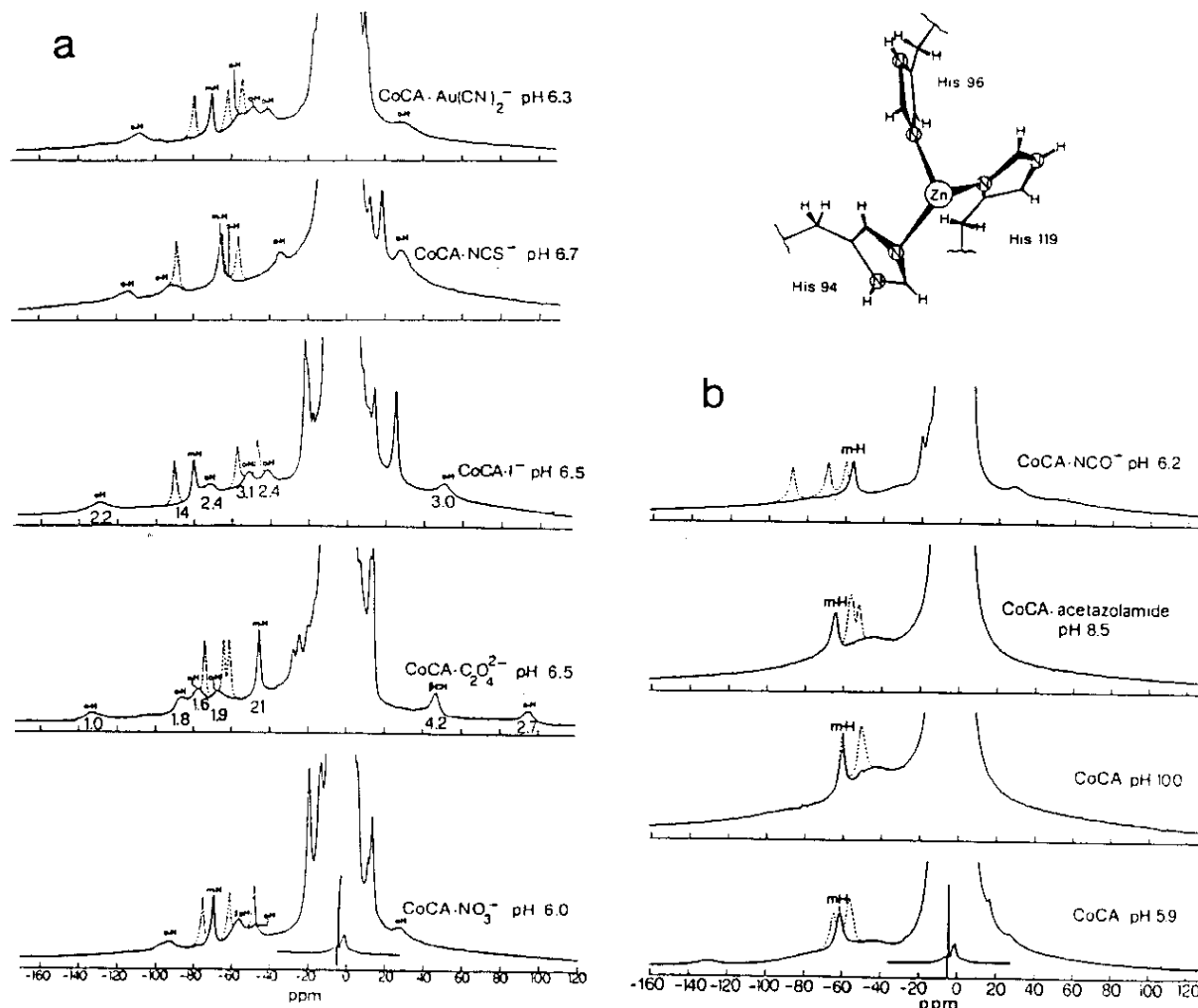


Figure 12. Historical 60 MHz  $^1\text{H}$  NMR spectra of 5-coordinated (a) and 4-coordinated (b) cobalt(II)-substituted carbonic anhydrase derivatives. The relatively sharp downfield lines visible in both groups of derivatives belong to the meta-like ring NH and CH protons of the three metal-coordinated histidines (inset). The broader signals belonging to ortho-like histidine ring protons are much more apparent in the spectra of the 5-coordinated derivatives in (b) <sup>60</sup>.

## 5.2. Relaxation reagents

Relaxation reagents are those metal ions or their complexes or radicals which provide broadening much more than shifts. Generally, relaxation reagents have a ground state spin multiplet with excited states far away. Therefore they have little or no magnetic anisotropy and the hyperfine shifts are mainly contact in origin. After a few chemical bonds the hyperfine shifts vanish, whereas line broadening, which is dramatic on nearby nuclei, can be observed very far (up to 20-25 Å) from

where the electron mainly resides. Gadolinium(III), manganese(II), copper(II) and chromium(III) are typical relaxation reagents. They permit distance estimates and then mapping. Since the pioneering works of Cohn <sup>71</sup>, Mildvan <sup>71,72</sup>, Navon <sup>73</sup> and others, this practice has become widespread in the investigation of biological molecules. The advent of bidimensional NMR has reduced the impact of this approach which, in principle, is still very useful. The broadening of the proton signals of a polynucleotide to which a platinum complex containing a spin label was attached has been used to build a model of the polynucleotide structure <sup>74</sup>. Recently, the relaxation properties have been exploited also in the case of shift reagents as further structural constraints (see Chapter 10), or to build structural models <sup>75-77</sup>.

### 5.3. Contrast agents in MRI

MRI reveals the presence of different NMR properties in different regions of the investigated object. The nucleus to be monitored is typically <sup>1</sup>H. Either its concentration, or relaxation properties, or both are monitored. Relaxation is a very sensitive parameter because it is related to water mobility at the extra- and intracellular level. Paramagnetic metal ions cause nuclear relaxation enhancements and therefore can increase contrast in an image if they distribute differently in different regions of the sample. Compounds with this property are called contrast agents <sup>78</sup>. Gadolinium(III) complexes are typical contrast agents <sup>79</sup>. The first commercially available contrast agent is Gd-DTPA (**Figure 13**). Gadolinium(III) is poisonous as metal ion but not if complexed <sup>80</sup>. Ideally, the complex should be excreted just after the time needed for the measurements.

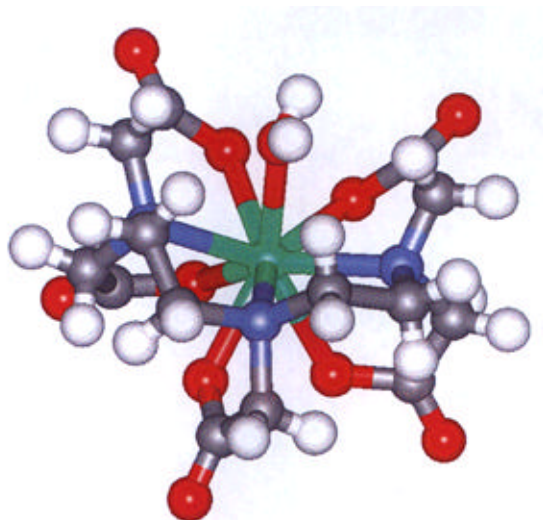


Figure 13. Ball-and-stick representation of the  $\text{Gd}(\text{DTPA})^{2-}$  complex <sup>111,112</sup>. The metal is coordinated by three amine nitrogens, five monodentate carboxylates and one water molecule.

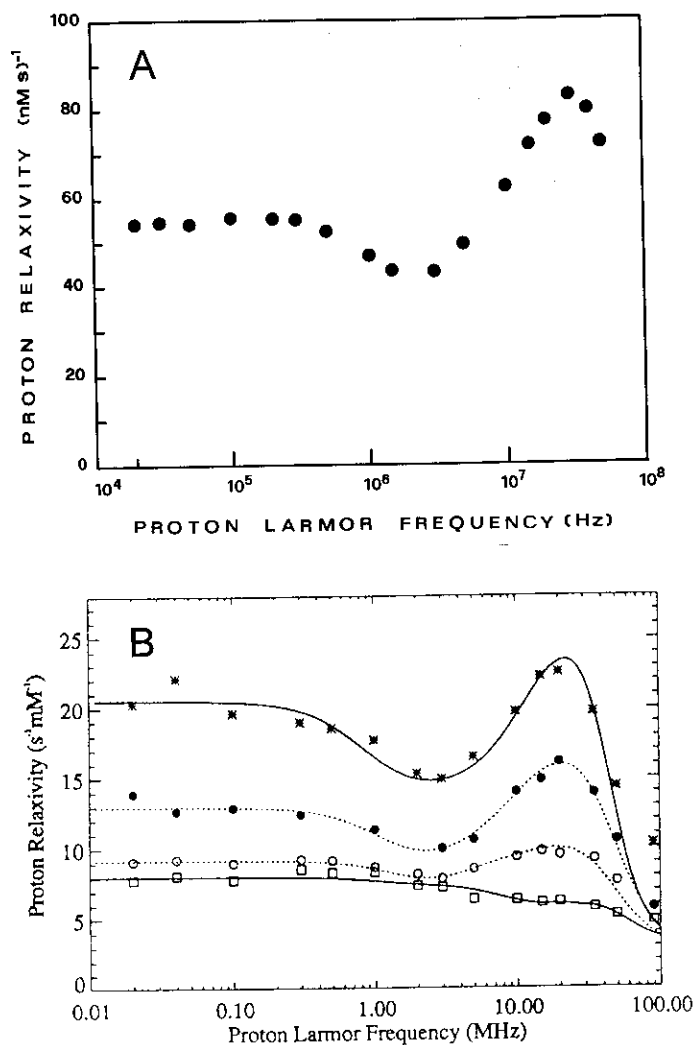


Figure 14. A) Proton relaxivity of gadolinium(III)-substituted concanavalin A <sup>81</sup> and B) of the contrast agent Gd(BOPTA)<sup>2-</sup> (a derivative of Gd(DTPA)<sup>2-</sup> in cross-linked bovine serum albumin solution (upper curve) <sup>83</sup>.

The gadolinium(III) complex should have at least a water molecule which exchanges rapidly with bulk water. The aqua-gadolinium water proton relaxation properties have been discussed (see Section 4.). When the gadolinium complex interacts with a tissue or a protein, then the relaxation properties become those typical of a gadolinium protein (see **Figure 14**) with a bell-shaped profile <sup>50,81-83</sup>. At the field of maximal relaxation the efficiency as contrast agent is enhanced. Strategies have been developed to increase the affinity of the gadolinium complex for tissues or to attach the gadolinium complex to a pendant which specifically binds to a protein. An interesting application is that of using as potential contrast agent a coordinatively saturated gadolinium(III) complex

whose ligand can be partially hydrolyzed by specific enzymes, making a coordination position available to a water molecule (**Figure 15**)<sup>86</sup>. Contrast can be thereby turned on when the specific target tissue containing the enzyme is reached.

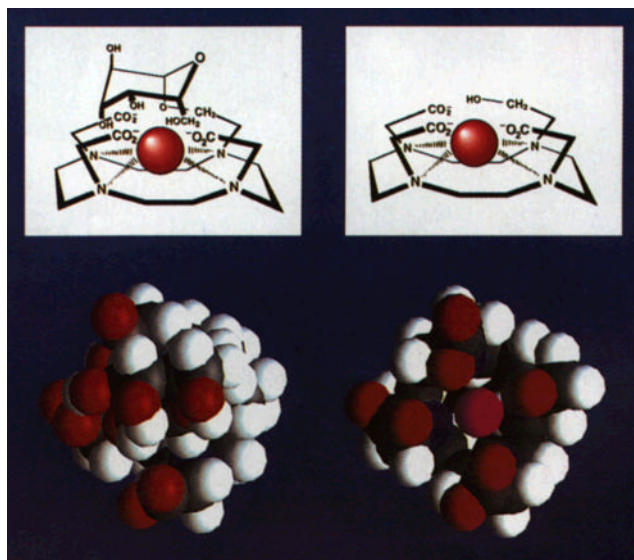


Figure 15. A stereoview of a derivative of  $\text{Gd}(\text{DOTA})^{-113}$  functionalized with a galactopyranoside “lid” that blocks the access of water (top)<sup>86</sup>. In the presence of  $\beta$ -galactosidase activity the “lid” is removed (bottom), water has access to the paramagnetic center and contrast is enhanced.

## 6. Magnetic coupled systems

Di- and polymetallic systems are common in proteins. Sometimes an atom or an aromatic ligand bridge two metal ions and provide a pathway for electron spin-electron spin interaction. This interaction affects electronic energy levels and relaxation rates. In turn, changes are induced in nuclear relaxation rates and hyperfine shifts. After observing in 1984 the  $^1\text{H}$  NMR signals of the  $\beta$ - $\text{CH}_2$  of the cysteines coordinated to both iron(II) and iron(III) in reduced  $\text{Fe}_2\text{S}_2$  ferredoxin<sup>87</sup>, in 1985 the  $^1\text{H}$  NMR spectra of the cobalt-substituted copper-zinc superoxide dismutase ( $\text{Cu}_2\text{Co}_2\text{SOD}$ )<sup>88</sup>, and after recognizing that in both cases such observations were possible thanks to magnetic coupling, we have devoted much attention to the consequences of magnetic coupling in NMR spectroscopy. A pioneering work by Palmer et al. dating back to 1971 attempted to explain the  $^1\text{H}$  NMR spectra of  $\text{Fe}_2\text{S}_2$  ferredoxins<sup>89</sup>.

Let us consider a dimetallic system whose magnetic coupling interaction is given by:

$$H = JS_1 S_2 \quad (31)$$

where  $J$  is the isotropic coupling constant and 1 and 2 refer to the two metal ions. If  $S_2$  is a metal ion with fast electron relaxation, it causes a relaxation enhancement of the slow-relaxing ion  $S_1$ . If  $J < \hbar\tau_{s_2}^{-1}$ , the problem can be afforded through perturbation theory<sup>90</sup> and the following equation is derived<sup>38</sup>:

$$\tau_{s_1}^{-1}(J) = \tau_{s_1}^{-1}(0) + \frac{2}{3}S_2(S_2 + 1) \frac{J^2}{\hbar} \frac{\tau_{s_2}}{1 + (\omega_{s_1} - \omega_{s_2})^2 \tau_{s_2}^2} \quad (32)$$

where  $\tau_{s_1}^{-1}(J)$  is the electronic relaxation rate of metal ion  $S_1$  in the coupled system,  $\tau_{s_1}^{-1}(0)$  is the electronic relaxation rate of metal ion  $S_1$  in the absence of coupling, and the second term on the right hand side is the electronic relaxation rate enhancement due to coupling to  $S_2$ . The relaxation rate of  $S_2$  remains unaltered. When  $J \approx \hbar\tau_{s_2}^{-1}$ , **Equation 32** breaks down and the transition probabilities between  $M_S$  values are common to both ions. As in the case of single metal ions with  $S > 1$ , it may be reasonable to assume a single effective  $\tau_s$  value for the whole system as far as nuclear relaxation is concerned.

In the case of dipolar  $S_1$ - $S_2$  coupling, the treatment is similar. The coupling energy is never very large, as it decreases with  $r^{-6}$ . In a frozen system the relaxation time of metal ion 1 is given by<sup>91-93</sup>:

$$\tau_{s_1}^{-1}(J) = \tau_{s_1}^{-1}(0) + \frac{\mu_0^2}{4\pi} \frac{1}{\hbar} \frac{g_e^4 \mu_B^4 S_2(S_2 + 1)}{\langle r^3 \rangle^2} \frac{a^2 \tau_{s_2}}{1 + (\omega_{s_1} + \omega_{s_2})^2 \tau_{s_2}^2} + \frac{b^2 \tau_{s_2}}{1 + \omega_{s_1}^2 \tau_{s_2}^2} + \frac{c^2 \tau_{s_2}}{1 + (\omega_{s_1} - \omega_{s_2})^2 \tau_{s_2}^2} \quad (33)$$

where  $a^2 = \frac{3}{2} \sin^4 \theta$ ,  $b^2 = \frac{3}{4} \sin^2 2\theta$ , and  $c^2 = \frac{1}{6} (3 \cos^2 \theta - 1)^2$ , and  $\theta$  is the angle between the  $S_1$ - $S_2$  vector and the external magnetic field, whereas its average in solution is<sup>38</sup>:

$$\tau_{s1}^{-1}(J) = \tau_{s1}^{-1}(0) + \frac{2}{15} \frac{\mu_0}{4\pi} \frac{1}{\hbar} \frac{g_e^4 \mu_B^4 S_2(S_2 + 1)}{\langle r^3 \rangle^2} \frac{6\tau_{s2}}{1 + (\omega_{s1} + \omega_{s2})^2 \tau_{s2}^2} + \frac{3\tau_{s2}}{1 + \omega_{s1}^2 \tau_{s2}^2} + \frac{\tau_{s2}}{1 + (\omega_{s1} - \omega_{s2})^2 \tau_{s2}^2} \quad (34)$$

When the two metal ions are equal and in similar environments,  $\tau_{s1}(0) = \tau_{s2}(0)$ , no increase in electronic relaxation rates is expected upon coupling on the basis of the above reasoning, as found for example in the protein Cu,Zn superoxide dismutase where zinc has been substituted with copper<sup>94</sup>. However, in every magnetic coupled system new electronic relaxation mechanisms may occur which shorten the overall electronic correlation time<sup>95</sup>. This has been observed in other dicopper complexes<sup>96,97</sup> and it is probable that it occurs in polymetallic centers like Fe-S proteins<sup>98-100</sup>. The general conclusion is that magnetic coupling causes enhancement in the electronic relaxation rates of the slow relaxing metal ion. If  $J \gg \hbar\tau_{s2}^{-1}$ , then there is a single electronic correlation time which is as short as  $\tau_{s2}$  or shorter. Consequently, the conditions to perform high resolution NMR are greatly improved.

After discussing the electronic relaxation times, the effects of hyperfine coupling on the hyperfine shifts and hyperfine relaxation should be revisited following the treatment in 2. We have now several energy levels arising from Hamiltonian 31. For example, in a  $S_1=1/2$ ,  $S_2=3/2$  antiferromagnetically ( $J > 0$ ) coupled system, we have two levels with  $S'$  (total  $S$ ) equal 1 and 2 separated by  $J$ , as shown in **Figure 16**.

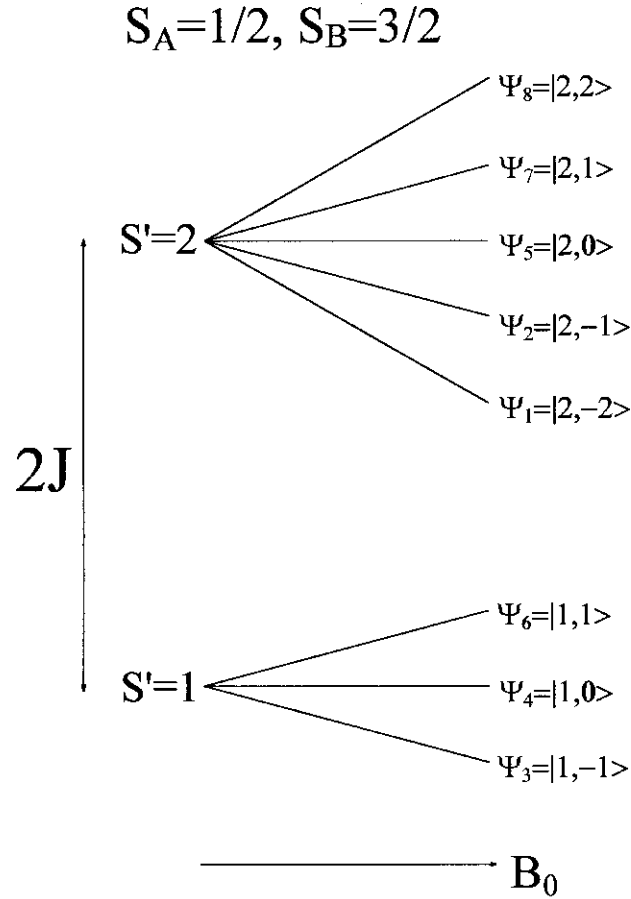


Figure 16. The new  $S' = 1$  and  $S' = 2$  states originated by magnetic exchange coupling between an  $S_A = 1/2$  and  $S_B = 3/2$  ions. The two new states are split into their  $M_s$  components by the magnetic field  $B_0$  and are separated by the exchange coupling constant  $J$  at zero field.

Nuclei interact with both levels. The contact shift involving nuclei interacting, for instance, with metal ion 1 and level 1 can be expressed as a function of  $\langle S_{1z} \rangle$  projected out from the  $S'=1$  level ( $\langle S_{1z} \rangle_1$ ) and of the hyperfine coupling  $A_1$  of the uncoupled system, i.e.

$$\delta^{con} = A_1 \langle S_{1z} \rangle_1 \quad (35)$$

or as a function of total  $\langle S_z' \rangle_1$  and a new coupling constant  $A_1'$ :

$$\delta^{con} = A_1' \langle S_z' \rangle_1 \quad (36)$$

By equating the two equations we obtain:

$$A_i' = A_1 \frac{\langle S_{1z} \rangle_1}{\langle S_z \rangle_1} = A_1 C_{11} \quad (37)$$

In general <sup>101-103</sup>,

$$A_{ni}' = A_n \frac{\langle S_{nz} \rangle_i}{\langle S_z \rangle_i} = A_n C_{ni} \quad (38)$$

where  $n$  refers to the metal ion and  $i$  to the level. Since  $A_n$  can be taken from an analogous system without magnetic coupling,  $\langle S_z \rangle_i = \frac{g_e \mu_B S_i' (S_i' + 1) B_0}{3kT}$ , and  $\langle S_{nz} \rangle_i$  can be computed using Hamiltonian 31 and standard projection techniques, the four parameters are known. **Equation 38** is valid for any level in any magnetically coupled polymetallic center. Coming back to the  $S_1 = 1, S_2 = 3/2$  example, the total shift is obtained by summing the contribution of the  $S' = 1$  and  $S' = 2$  levels:

$$\delta^{con} = \frac{A_{11}' \langle S_z \rangle_1 + A_{12}' \langle S_z \rangle_2 \exp(-J/kT)}{1 + \exp(-J/kT)} \quad (39)$$

where the exponential introduces the Boltzmann population. In general,

$$\delta^{con} = A_1 \frac{g_e \mu_B}{\hbar \gamma_I 3kT} \frac{C_i S_i' (S_i' + 1) (2S_i' + 1) \exp(-E_i/kT)}{(2S_i' + 1) \exp(-E_i/kT)} \quad (40)$$

where  $i$  is referred to all levels. Note that if  $J \ll kT$ , all the levels are equally populated and the sum of the projections of  $\langle S_{1z} \rangle_i$  is just  $\langle S_{1z} \rangle$ . In other words, if  $J \ll kT$  the shifts are not affected by magnetic coupling <sup>88</sup>. For pseudocontact shifts no formal treatment is available, but when  $J \ll kT$  the consequences of magnetic coupling are the same.

In cobalt(II)-substituted copper-zinc superoxide dismutase (CuCoSOD) where  $J = 17 \text{ cm}^{-1}$  (**Figure 17**) the shifts are just the same of those of the two separate ions<sup>88</sup>, whereas in reduced two iron-two sulfur ferredoxins containing the  $[\text{Fe}_2\text{S}_2]^+$  cluster (**Figure 18**) ( $J = 300 \text{ cm}^{-1}$ ,  $kT$ ), the spectra and their temperature dependencies are accounted for by **Equation 40**<sup>87,99,100,104-107</sup>.

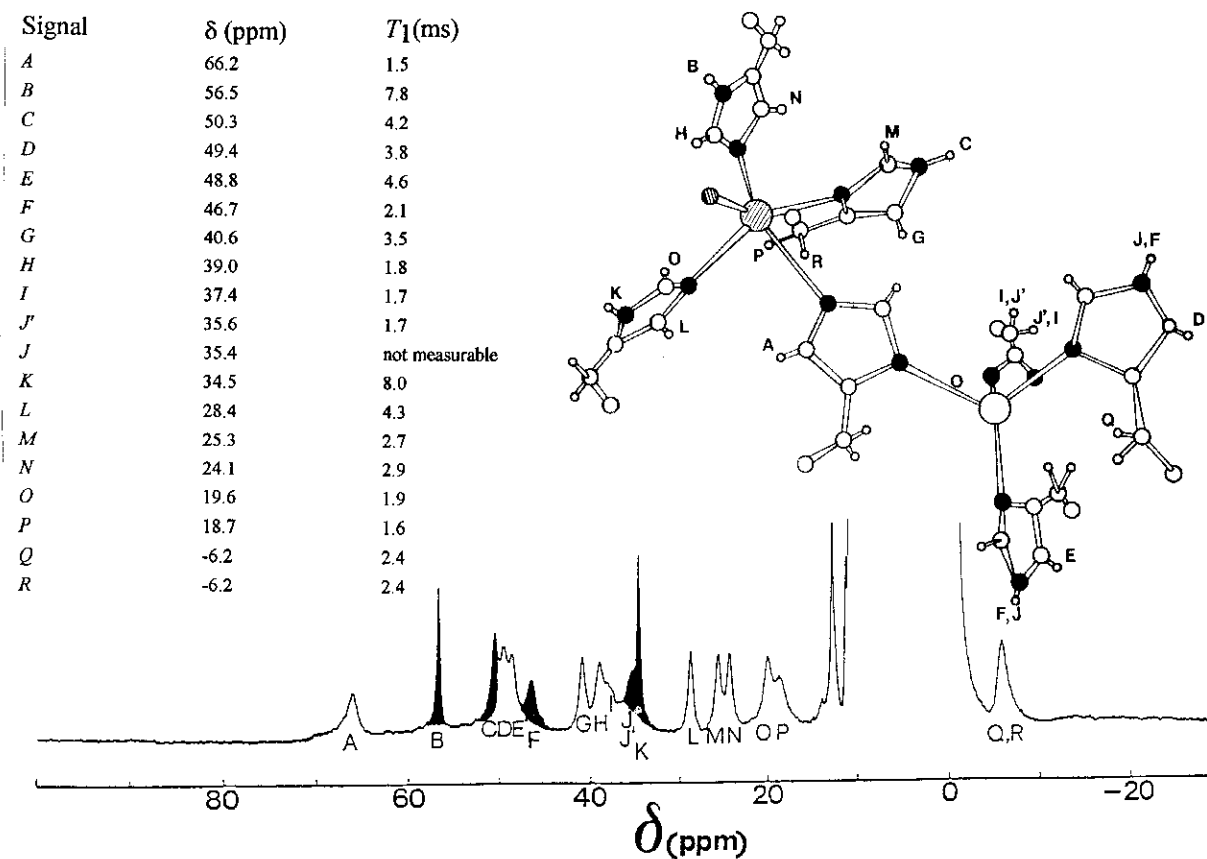


Figure 17. 300 MHz  $^1\text{H}$  NMR spectrum of  $\text{Cu}_2\text{Co}_2\text{SOD}$ <sup>88,108</sup>, with signal assignment and schematic drawing of the active site (Cu = shaded sphere, Co = hollow sphere).

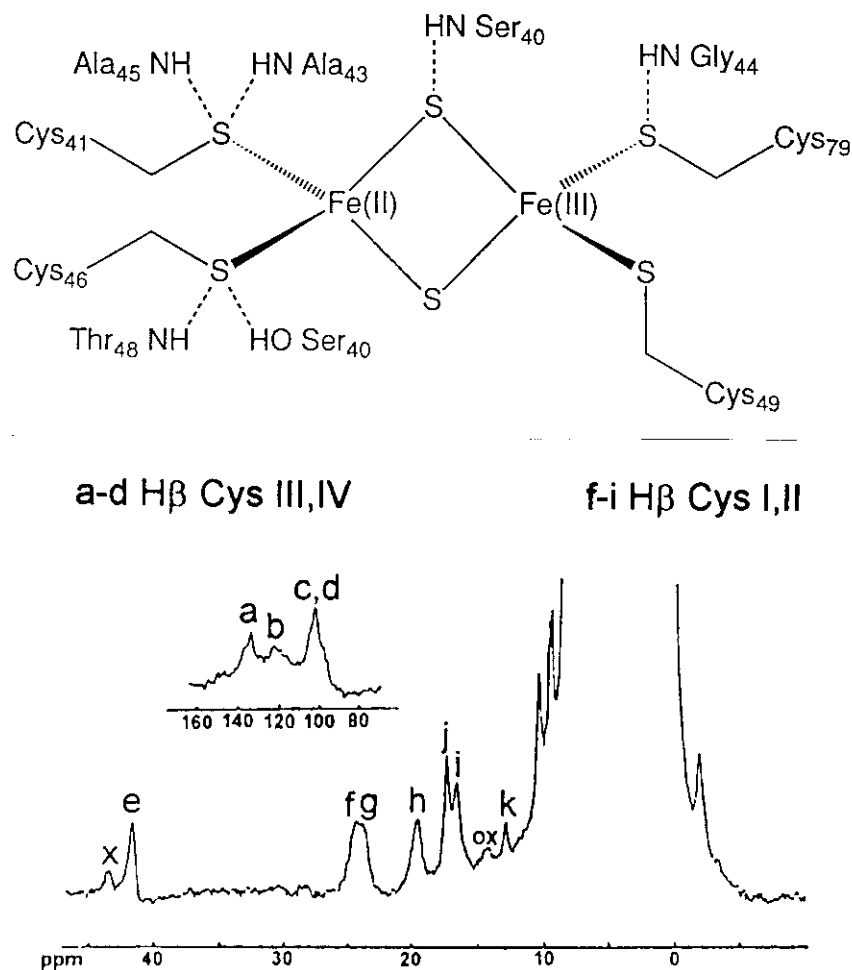


Figure 18. Historical 200 MHz  $^1\text{H}$  NMR spectrum of reduced spinach ferredoxin. Signals a-d belong to  $-\text{CH}_2$  protons of the third and fourth cysteines in the sequence (Cys-49 and Cys-79), coordinated to the ferric ion, and signals f-i to the first and second cysteine in the sequence (Cys-41 and Cys-46) coordinated to the ferrous ion<sup>87,114</sup>.

As far as nuclear relaxation is concerned, it has already been noticed that  $\tau_c$  is shortened, and this may affect the total  $\tau_c$  according to **Equation 18**. The hyperfine relaxation depends on the average squared energy  $\langle E^2 \rangle$  which depends on  $\langle A^2 \rangle$  for contact relaxation and on  $\left\langle \frac{\mu_I \mu_S}{r^3} \right\rangle^2$  for dipolar relaxation, where  $\mu_I$  and  $\mu_S$  are the nuclear and electronic magnetic moments, respectively. Of course,  $\mu_{S1}^2$  is proportional to  $S_1(S_1 + 1)$  of metal ion 1 of each  $i$  level, and therefore to  $C_{1i}^2$ . Such coefficients, which apply to **Equations 11-13** and **15-17**, lead to a further

decrease in nuclear relaxation and linewidth. For example, in **Table 3** the relaxation parameters for CuCoSOD<sup>108</sup> and [Fe<sub>2</sub>S<sub>2</sub>]<sup>+</sup> containing ferredoxins<sup>38</sup> are reported<sup>95,109</sup>.

Table 3. Electron relaxation times  $\tau_s$  (s) for Cu<sub>2</sub>Co<sub>2</sub>SOD and [Fe<sub>2</sub>S<sub>2</sub>]<sup>+</sup> ferredoxin.

Copper(II)	Cu <sup>II</sup> , monomeric, in Cu <sub>2</sub> Zn <sub>2</sub> SOD	Cu <sup>II</sup> , coupled to Co <sup>II</sup> in Cu <sub>2</sub> Co <sub>2</sub> SOD
	$2 \times 10^{-9}$	$1 \times 10^{-11}$
Cobalt(II)	Co <sup>II</sup> , monomeric, in Cu <sub>2</sub> Co <sub>2</sub> SOD	Co <sup>II</sup> , coupled to Cu <sup>II</sup> in Cu <sub>2</sub> Co <sub>2</sub> SOD
	$1 \times 10^{-11}$	$5 \times 10^{-12}$
Iron(II)	Fe <sup>II</sup> , monomeric, in rubredoxin	Fe <sup>II</sup> , coupled to Fe <sup>III</sup> in ferredoxin
	$5 \times 10^{-11}$	$2 \times 10^{-12}$
Iron(III)	Fe <sup>III</sup> , monomeric, in rubredoxin	Fe <sup>III</sup> , coupled to Fe <sup>III</sup> in ferredoxin
	$1 \times 10^{-9}$	$2 \times 10^{-12}$

As already noted, in the cases of  $S' > 1$  levels, several electronic transitions are possible, each one with its own probability of course for each  $S'$  level. Therefore, there are several relaxation times; however, the nuclear relaxation properties can again be simulated with a single electronic correlation time. Furthermore, some levels arising from Hamiltonian 31 may be only partially populated. A treatment for  $S_1=1/2$  and  $S_2=1/2, 1$  and  $3/2$  is available in the literature<sup>109</sup>, and shows that the overall electronic correlation time is one for the system and close to  $\tau_{s2}$ .

Note that when two metal ions are equal, all  $C_{ni}$  equal  $1/2$ . When the two metal ions are different and antiferromagnetically coupled, the  $C_{n1}$  of the  $n$  ion with larger spin is positive, whereas that with the smaller spin is negative. That means that if  $J \gg kT$  and only the ground state is populated, the shifts of the nuclei sensing the metal ion with larger  $S$  will have the same sign as in uncoupled systems whereas the shifts of the nuclei of the other domain will have reverse sign

21,104,105. Since when all the levels are equally populated the shifts of both domains are the same as those of the uncoupled systems, the shifts of the ion with smaller  $S$  will be highly variable. **Figure 19** accounts for the observations in the  $[\text{Fe}_2\text{S}_2]^+$  case. The occurrence of magnetic coupling is signaled by the strong and unusual dependence on temperature of the shifts of nuclei belonging to the small  $S$  domain<sup>99</sup>. In fact, the temperature affects the population of the levels. A decrease in temperature will increase the weight of the ground state and will move the shifts of nuclei of the small  $S$  ion upfield (**Figure 19**, right). In the case of  $[\text{Fe}_2\text{S}_2]^+$ ,  $\text{Fe}^{3+}$  has  $S = 5/2$  and  $\text{Fe}^{2+}$  has  $S = 2$ . Signals f, g, h and i, assigned to  $-\text{CH}_2$  protons of the cysteines bound to  $\text{Fe}^{2+}$ , move upfield when the temperature is decreased (**Figure 19**, left)<sup>87,89</sup>.

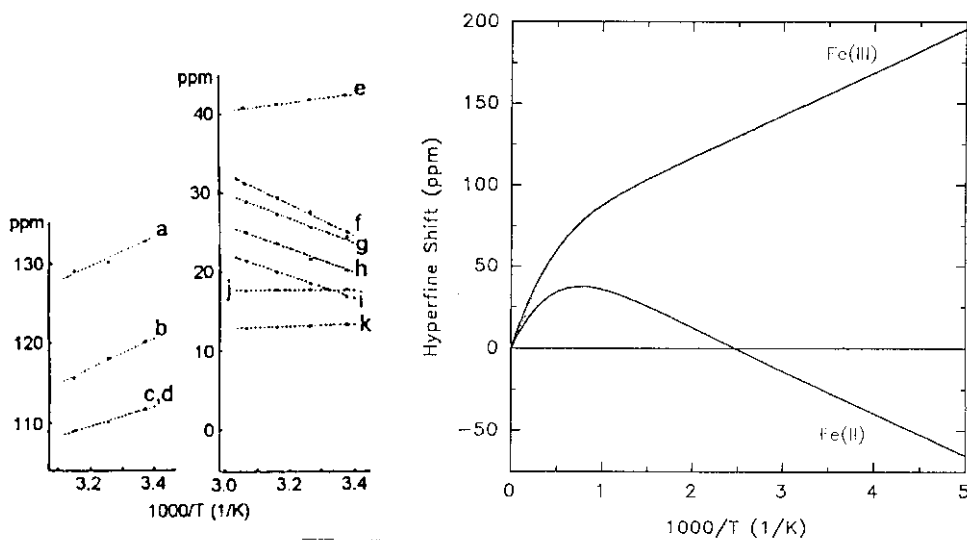


Figure 19. Observed (left)<sup>87</sup> and calculated (right)<sup>100</sup> temperature dependences of the hyperfine shifts of the  $-\text{CH}_2$  protons of coordinated cysteines in reduced spinach ferredoxin (Figure 18). The theoretical temperature dependence is calculated using  $J = 200 \text{ cm}^{-1}$  and  $A/h = 1.8 \text{ MHz}$  for the isolated ions.

## Bibliography

- (1) Stevens, K. W. H. *Phys. Rep.* **1976**, *24c*, 1-75.
- (2) Abragam, A.; Bleaney, B. *Electron Paramagnetic Resonance of Transition Metal Ions*; Clarendon Press: Oxford, 1970;
- (3) Griffith, J. S. *The theory of transition-metal ions*; Cambridge University Press: Cambridge, 1961;
- (4) Rubinstein, M.; Baram, A.; Luz, Z. *Mol. Phys.* **1971**, *20*, 67-80.
- (5) Halle, B. *Progr. NMR Spectrosc.* **1996**, *28*, 137-159.
- (6) Bruschiweiler, R.; Case, D. A. *Phys. Rev. Lett.* **1994**, *72*, 940-943.
- (7) Abragam, A. *The Principles of Nuclear Magnetism*; Oxford University Press: Oxford, 1961;
- (8) McConnell, H. M.; Chesnut, D. B. *J. Chem. Phys.* **1958**, *28*, 107-117.
- (9) Fermi, E. *Z. Phys.* **1930**, *60*, 320
- (10) Jesson, J. P. In *NMR of paramagnetic molecules*; La Mar, G. N., Horrocks, W. D., Jr., Holm, R. H. Eds.; Academic Press: New York, 1973; pp 1-52.
- (11) Kurland, R. J.; McGarvey, B. R. *J. Magn. Reson.* **1970**, *2*, 286-301.
- (12) McConnell, H. M.; Robertson, R. E. *J. Chem. Phys.* **1958**, *29*, 1361-1365.
- (13) Gottlieb, H. P. W.; Barfield, M.; Doddrell, D. M. *J. Chem. Phys.* **1977**, *67*, 3785-3794.
- (14) Doddrell, D. M.; Healy, P. C.; Bendall, M. R. *J. Magn. Reson.* **1978**, *29*, 163
- (15) Bloembergen, N. *J. Chem. Phys.* **1957**, *27*, 575-596.
- (16) Koenig, S. H. *J. Magn. Reson.* **1982**, *47*, 441-453.
- (17) Solomon, I. *Phys. Rev.* **1955**, *99*, 559-565.
- (18) Koenig, S. H. *J. Magn. Reson.* **1978**, *31*, 1-10.
- (19) Gueron, M. *J. Magn. Reson.* **1975**, *19*, 58-66.
- (20) Vega, A. J.; Fiat, D. *Mol. Phys.* **1976**, *31*, 347-355.

- (21) Bertini, I.; Luchinat, C. *NMR of paramagnetic substances*; Coord.Chem.Rev. 150, Elsevier: Amsterdam, 1996; pp 1-300.
- (22) Bertini, I.; Luchinat, C.; Macinai, R.; Piccioli, M.; Scozzafava, A.; Viezzoli, M. S. *J. Magn. Reson. Ser. B* **1994**, *B104*, 95-98.
- (23) Koenig, S. H.; Schillinger, W. E. *J. Biol. Chem.* **1969**, *244*, 3283-3280.
- (24) Koenig, S. H.; Schillinger, W. E. *J. Biol. Chem.* **1969**, *244*, 6520-6526.
- (25) Bertini, I.; Galas, O.; Luchinat, C.; Parigi, G. *J. Magn. Reson. Ser. A* **1995**, *113*, 151-158.
- (26) Larsson, T.; Westlund, P.-O.; Kowalewski, J.; Koenig, S. H. *J. Chem. Phys.* **1994**, *101*, 1116
- (27) Svoboda, J.; Nilsson, T.; Kowalewski, J.; Westlund, P.-O.; Larsson, P. T. *J. Magn. Reson. Ser. A* **1996**, *121*, 108
- (28) Sharp, R. R. *J. Chem. Phys.* **1993**, *98*, 2507
- (29) Bertini, I.; Luchinat, C.; Mancini, M.; Spina, G. *J. Magn. Reson.* **1984**, *59*, 213-222.
- (30) Bertini, I.; Luchinat, C.; Kowalewski, J. *J. Magn. Reson.* **1985**, *62*, 235-241.
- (31) Bayburt, T.; Sharp, R. R. *J. Chem. Phys.* **1990**, *92*, 5892-5899.
- (32) Bertini, I.; Luchinat, C. *NMR of paramagnetic molecules in biological systems*; Benjamin/Cummings: Menlo Park, CA, 1986;
- (33) Nordenskiöld, L.; Laaksonen, L.; Kowalewski, J. *J. Am. Chem. Soc.* **1982**, *104*, 379-382.
- (34) Bertini, I.; Briganti, F.; Luchinat, C.; Mancini, M.; Spina, G. *J. Magn. Reson.* **1985**, *63*, 41-55.
- (35) Kowalewski, J.; Nordenskiöld, L.; Benetis, N.; Westlund, P.-O. *Progr. NMR Spectrosc.* **1985**, *17*, 141-185.
- (36) Kowalewski, J.; Larsson, T.; Westlund, P.-O. *J. Magn. Reson.* **1987**, *74*, 56-65.
- (37) Hertz, H. G. *Water: A Comprehensive Treatise Vol.3*; Plenum Press: New York, 1973;
- (38) Banci, L.; Bertini, I.; Luchinat, C. *Nuclear and electron relaxation. The magnetic nucleus-unpaired electron coupling in solution*; VCH: Weinheim, 1991;
- (39) Kennedy, S. D.; Bryant, R. G. *Magn. Reson. Med.* **1985**, *2*, 14-19.
- (40) Hernandez, G.; Tweedle, M.; Bryant, R. G. *Inorg. Chem.* **1990**, *29*, 5110-5113.

- (41) Bertini, I.; Briganti, F.; Luchinat, C.; Xia, Z. *J. Magn. Reson.* **1993**, *101*, 198-201.
- (42) Banci, L.; Bertini, I.; Luchinat, C. *Inorg. Chim. Acta* **1985**, *100*, 173-181.
- (43) Bloembergen, N.; Morgan, L. O. *J. Chem. Phys.* **1961**, *34*, 842-850.
- (44) Kivelson, D. *J. Chem. Phys.* **1966**, *45*, 1324-1332.
- (45) Koenig, S. H.; Brown III, R. D. *J. Magn. Reson.* **1985**, *61*, 426-439.
- (46) Banci, L.; Bertini, I.; Luchinat, C. *Magn. Reson. Rev.* **1986**, *11*, 1-40.
- (47) Muus, L. T.; Atkins, P. W. *Electronic Spin Relaxation in Liquids*; Plenum Press: New York, 1972;
- (48) Kivelson, D. *J. Chem. Phys.* **1964**, *41*, 1904-1909.
- (49) Bertini, I.; Luchinat, C.; Xia, Z. *J. Magn. Reson.* **1992**, *99*, 235-246.
- (50) O'Hara, P. B.; Koenig, S. H. *Biochemistry* **1986**, *25*, 1445-1450.
- (51) Bertini, I.; Galas, O.; Luchinat, C.; Messori, L.; Parigi, G. *J. Phys. Chem.* **1995**, *99*, 14217-14222.
- (52) Reuben, J. *J. Magn. Reson.* **1973**, *11*, 103-104.
- (53) Horrocks, W. D., Jr. In *NMR of paramagnetic molecules*; La Mar, G. N., Horrocks, W. D., Jr., Holm, R. H. Eds.; Academic Press: New York, 1973; pp 479-519.
- (54) Reuben, J.; Elgavish, G. A. *J. Magn. Reson.* **1980**, *39*, 421-430.
- (55) Jardetzky, O. *Biochim. Biophys. Acta* **1980**, *621*, 227
- (56) Lee, L.; Sykes, B. D. *Biochemistry* **1983**, *22*, 4366-4373.
- (57) Capozzi, F.; Cremonini, M. A.; Luchinat, C.; Sola, M. *Magn. Reson. Chem.* **1993**, *31*, S118-S127.
- (58) Bentrop, D.; Bertini, I.; Cremonini, M. A.; Forsén, S.; Luchinat, C.; Malmendal, A. *Biochemistry* **1997**, *36*, 11605-11618.
- (59) McDonald, C. C.; Phillips, W. D. *Biochem. Biophys. Res. Commun.* **1969**, *35*, 43
- (60) Bertini, I.; Luchinat, C. *Adv. Inorg. Biochem.* **1985**, *6*, 71-111.
- (61) Bertini, I.; Lanini, G.; Luchinat, C. *J. Am. Chem. Soc.* **1983**, *105*, 5116-5118.

- (62) Bertini, I.; Luchinat, C. *Acc. Chem. Res.* **1983**, *16*, 272-279.
- (63) Bertini, I.; Luchinat, C.; Pierattelli, R.; Vila, A. J. *Eur. J. Biochem.* **1992**, *208*, 607-615.
- (64) Bertini, I.; Luchinat, C.; Pierattelli, R.; Vila, A. J. *Inorg. Chem.* **1992**, *31*, 3975-3979.
- (65) Bertini, I.; Turano, P.; Vila, A. J. *Chem. Rev.* **1993**, *93*, 2833-2932.
- (66) Auld, D. S.; Bertini, I.; Donaire, A.; Messori, L.; Moratal Mascarell, J. M. *Biochemistry* **1992**, *31*, 3840-3846.
- (67) Salgado, J.; Jimenez, H. R.; Donaire, A.; Moratal, J. M. *Eur. J. Biochem.* **1995**, *231*(2), 358-369.
- (68) Bertini, I.; Canti, G.; Luchinat, C.; Scozzafava, A. *J. Am. Chem. Soc.* **1978**, *100*, 4873-4877.
- (69) Bertini, I.; Canti, G.; Luchinat, C.; Mani, F. *J. Am. Chem. Soc.* **1981**, *103*, 7784-7788.
- (70) Bertini, I.; Gerber, M.; Lanini, G.; Luchinat, C.; Maret, W.; Rawer, S.; Zeppezauer, M. *J. Am. Chem. Soc.* **1984**, *106*, 1826-1830.
- (71) Cohn, M.; Mildvan, A. S. *Adv. Enzymol.* **1970**, *33*, 1
- (72) Mildvan, A. S. *Acc. Chem. Res.* **1977**, *10*, 246
- (73) Lanir, A.; Navon, G. *Biochemistry* **1972**, *11*, 3536
- (74) Dunham, S. U.; Lippard, S. J. *J. Am. Chem. Soc.* **1995**, *117*, 10702-10712.
- (75) Modi, S.; Paine, M. J.; Sutcliffe, M. J.; Lian, L. Y.; Primrose, W. U.; Wolf, C. R.; Roberts, G. C. *Biochemistry* **1996**, *35*, 4540-4550.
- (76) Oliver, C. F.; Modi, S.; Sutcliffe, M. J.; Primrose, W. U.; Lian, L. Y.; Roberts, G. C. *Biochemistry* **1997**, *36*, 1567-1572.
- (77) Poli-Scaife, S.; Attias, R.; Dansette, P. M.; Mansuy, D. *Biochemistry* **1997**, *36*, 12672-12682.
- (78) Lauffer, R. B. *Chem. Rev.* **1987**, *87*, 901
- (79) Aime, S.; Barbero, L.; Botta, M. *Magn. Res. Imaging* **1991**, *9*, 843-847.
- (80) Weinmann, H.-J.; Mühler, A.; Radüchel, B. In *Encyclopedia of Nuclear Magnetic Resonance*; Grant, D. M., Harris, R. K. Eds.; John Wiley & Sons: New York, 1996; pp 2166-2173.
- (81) Koenig, S. H.; Brown III, R. D. *Invest. Radiol. (Suppl. 2)* **1985**, *20*, 297

- (82) Cavagna, F. M.; Luchinat, C.; Scozzafava, A.; Xia, Z. *Magn. Res. Med.* **1994**, *31*, 58-60.
- (83) Bertini, I.; Luchinat, C.; Parigi, G.; Quacquareni, G.; Marzola, P.; Cavagna, F. M. *Magn. Res. Med.* **1998**, *39*, 124-131.
- (84) Cavagna, F. M.; Marzola, P.; Daprà, M.; Maggioni, F.; Vicinanza, E.; Castelli, P. M.; De Haen, C.; Luchinat, C.; Wendland, M. F.; Saeed, M.; Higgins, C. B. *Invest. Radiol. (Suppl. 2)* **1994**, *29*, S50-S53.
- (85) Bertini et al., in preparation
- (86) Moats, R. A.; Frazer, S. E.; Meade, T. J. *Angew. Chem. Int. (Ed. Engl. )* **1997**, *36*, 726-728.
- (87) Bertini, I.; Lanini, G.; Luchinat, C. *Inorg. Chem.* **1984**, *23*, 2729-2730.
- (88) Bertini, I.; Lanini, G.; Luchinat, C.; Messori, L.; Monnanni, R.; Scozzafava, A. *J. Am. Chem. Soc.* **1985**, *107*, 4391-4396.
- (89) Dunham, W. R.; Palmer, G.; Sands, R. H.; Bearden, A. J. *Biochim. Biophys. Acta* **1971**, *253*, 373-384.
- (90) Bertini, I.; Lanini, G.; Luchinat, C.; Mancini, M.; Spina, G. *J. Magn. Reson.* **1985**, *63*, 56-63.
- (91) Bloembergen, N. *Physica* **1949**, *15*, 386
- (92) Abragam, A. *Phys. Rev.* **1955**, *98*, 1729
- (93) Makinen, M. W.; Wells, G. B. In *Metal Ions in Biological Systems*, Vol. 22; Sigel, H. Ed.; Marcel Dekker: New York, 1987; pp 129-206.
- (94) Bertini, I.; Banci, L.; Brown III, R. D.; Koenig, S. H.; Luchinat, C. *Inorg. Chem.* **1988**, *27*, 951-953.
- (95) Clementi, V.; Luchinat, C. *Accounts of Chemical Research* **1998**, in press.
- (96) Murthy, N. N.; Karlin, K. D.; Bertini, I.; Luchinat, C. *J. Am. Chem. Soc.* **1997**, *119*, 2156-2162.
- (97) Lin, L.-Y.; Park, H. I.; Ming, L.-J. *JBIC* **1997**, *2*, 744-749.
- (98) Bertini, I.; Luchinat, C.; Mincione, G.; Soriano, A. *Inorg. Chem.* **1998**, in press.
- (99) Bertini, I.; Luchinat, C.; Soriano, A. *ACS series* **1998**, in press.
- (100) Bertini, I.; Ciurli, S.; Luchinat, C. *Struct. Bonding* **1995**, *83*, 1-54.

- (101) Noodleman, L. *Inorg. Chem.* **1988**, *27*, 3677-3679.
- (102) Noodleman, L. *Inorg. Chem.* **1991**, *30*, 256-264.
- (103) Noodleman, L. *Inorg. Chem.* **1991**, *30*, 246-256.
- (104) Banci, L.; Bertini, I.; Luchinat, C. *Struct. Bonding* **1990**, *72*, 113-135.
- (105) Luchinat, C.; Ciurli, S. *Biological Magnetic Resonance* **1993**, *12*, 357-420.
- (106) Benini, S.; Ciurli, S.; Luchinat, C. *Inorg. Chem.* **1995**, *34*, 417-420.
- (107) Bertini, I.; Luchinat, C. In *Transition metal sulfur chemistry: biological and industrial significance*; Stiefel, E. I., Matsumoto, K. Eds.; ACS Symposium Series N. 653: Washington DC, 1996; pp 57-73.
- (108) Bertini, I.; Luchinat, C.; Piccioli, M. *Progr. NMR Spectrosc.* **1994**, *26*, 91-141.
- (109) Bertini, I.; Galas, O.; Luchinat, C.; Parigi, G.; Spina, G. *J. Magn. Reson.* **1998**, in press.
- (110) Bax, A.; Griffey, R. H.; Hawkins, B. L. *J. Magn. Reson.* **1983**, *55*, 301-315.
- (111) Carr, D. H. *Physiol. Chem. Phys. Med. NMR* **1984**, *16*, 160
- (112) Laniado, M.; Weinmann, H. J.; Schörner, W.; Felix, R.; Speck, U. *Physiol. Chem. Phys. Med. NMR* **1984**, *16*, 157
- (113) Bousquet, J. C.; Saini, S.; Stark, D. D.; Hahn, P. F.; Nigam, M.; Wittenberg, J.; Ferrucci, J. *Radiology* **1988**, *166*, 693
- (114) Dugad, L. B.; La Mar, G. N.; Banci, L.; Bertini, I. *Biochemistry* **1990**, *29*, 2263-2271.